

AD-A036 328

MASSACHUSETTS INST OF TECH LEXINGTON LINCOLN LAB
LASER DEVELOPMENT IN SUPPORT OF THE JUMPER PROGRAM FOR LASER IS--ETC(U)
DEC 76 A L MCWHORTER

F/G 20/5

F19628-76-C-0002

UNCLASSIFIED

ESD-TR-76-347

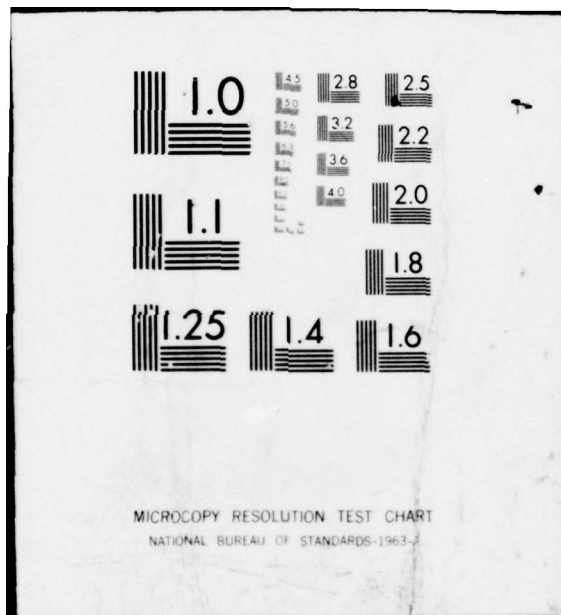
NL

1 OF 1
AD
A036328



END

DATE
FILMED
3-77



AD A 036328

Semiannual Report

Laser Development in Support of the JUMPer Program for Laser Isotope Separation

31 December 1976

Prepared by
Lincoln Laboratory
MASSACHUSETTS INSTITUTE OF TECHNOLOGY
LAWRENCE, MASSACHUSETTS



Approved for public release; distribution unlimited.



The work reported in this document was performed as a part of the research program in the Department of the Army, Office of the Chief of Staff, and the Department of the Army, Office of the Secretary of Defense, and the Department of the Army, Office of the Secretary of Defense, and the Department of the Army, Office of the Secretary of Defense.

The views and conclusions contained in this document are those of the author and should not be interpreted as necessarily representing the official policies, either expressed or implied, of the United States Government.

This technical report has been reviewed and is approved for publication.
FOR THE COMMANDER

Frederick J. Smith
Frederick J. Smith, Jr., USAF
Chief, USAF Library Technical Project Office

MASSACHUSETTS INSTITUTE OF TECHNOLOGY
LINCOLN LABORATORY

6
LASER DEVELOPMENT IN SUPPORT OF THE JUMPER PROGRAM
FOR LASER ISOTOPE SEPARATION.

10 Alan L. McWhorter

11 31 Dec 76

15 F19628-76-C-0002

12 69p.

9
SEMIANNUAL REPORT,
1 JUL 1976 - 31 DEC 1976.

ISSUED 18 JANUARY 1977

18 ESD

19 TR-76-347

Submitted to
Los Alamos Scientific Laboratory

D D C
RECEIVED
MAR 3 1977
A

Approved for public release; distribution unlimited.

LEXINGTON

MASSACHUSETTS

207 650

1473
mt

ABSTRACT

This report covers in detail the research and development work carried out by M. I. T. Lincoln Laboratory for the U. S. Energy Research and Development Administration in support of the JUMPer program at the Los Alamos Scientific Laboratory, during the period 1 July through 31 December 1976. The topics covered include optically pumped gas lasers, frequency calibration of the $^{14}\text{CO}_2$ laser, and microwave frequency shifting.

SEARCHED	INDEXED
SERIALIZED	FILED
JUL 1977	
FBI - NEW YORK	
A	

CONTENTS

Abstract

INTRODUCTION	1
1. 16 μm OPTICALLY PUMPED LASER	2
2. OPTICALLY PUMPED 7.75 AND 8.62 μm LASER DEVELOPMENT	8
3. CALIBRATION OF $^{14}\text{C}^{16}\text{O}_2$ LASER LINES	10
3-A Absolute Frequency Calibration of the CO_2 Isotope Lasers Transitions	13
3-B Advances in CO_2 Laser Stabilization Using the 4.3 μm Fluorescence Technique	37
4. MICROWAVE FREQUENCY SHIFTING	60

INTRODUCTION

Approximately one third of a millijoule of single pulse energy has been obtained from the optically pumped $16\text{ }\mu\text{m}$ CO_2 laser. In addition, grating tuning of the laser has resulted in single-line operation over a wide range of wavelengths in the $16\text{ }\mu\text{m}$ band. Finally, the entire $16\text{ }\mu\text{m}$ laser system including HBr pump lasers has been redesigned and rebuilt.

Preliminary measurements have been made of a number of $^{16}\text{O}^{13}\text{C}^{32}\text{S}$ laser transitions near $8.6\text{ }\mu\text{m}$. The threshold for this laser has been found to be 15 mJ in the present cavity configuration. The operating characteristics of the directly pumped $^{16}\text{O}^{12}\text{C}^{32}\text{S}$ laser have also been studied.

Absolute frequency calibration of the $^{14}\text{C}^{16}\text{O}_2$ laser transitions is currently under way. The data for absolute frequency calibration are obtained with a two-channel, line-center stabilized CO_2 laser heterodyne frequency calibration system. We have completed the measurements of about two dozen beat frequencies between the $^{14}\text{C}^{16}\text{O}_2$ $00^0_1 - [10^0_0, 02^0_0]_{\text{II}}$ band P and R transitions and adjacent $^{12}\text{C}^{16}\text{O}_2$ and $^{13}\text{C}^{18}\text{O}_2$ laser lines.

During the last six months a program was initiated to study the efficiency of shifting an infrared carrier at $10.6\text{ }\mu\text{m}$ by $\approx 15\text{ GHz}$ by means of the traveling wave linear electro-optic effect in either single-crystal GaAs or CdTe. The microwave and optical components have been assembled for the experiments. Initial microwave breakdown tests have been conducted to ascertain the peak microwave power that can be used in the microwave structures housing the mixing crystals.

1. 16 μ m OPTICALLY PUMPED LASER

During this reporting period, our work was concentrated in three general areas: understanding of the limiting kinetic processes in the optically pumped medium; improvements in the operation of this optically pumped laser (OPL); and redesign and rebuilding of each of the major laser components. As a result of this work, our OPL can now run reliably on a single line and with output energies which are practical for LASL applications.

Kinetic Processes in the OPL

One of the crucial questions regarding the kinetics of the OPL has been the relaxation of the upper level of the 16 μ m transition, designated $[10^00, 02^00]_{II}$. At the end of the last semiannual the relaxation of the lower laser level 01^10 was measured. Despite the fact that no other equi-energetic vibrational states exist for this level, the relaxation of this level by HBr is extremely fast $\sim 10^5 \text{ sec}^{-1} \text{ Torr}^{-1}$. This is apparently the result of vibrational to rotational (V-R) energy transfer. Obviously in the case of the upper level the same V-R mechanism should be operative. Further, since equi-energetic vibrational product channels are available (see Figure 1-1), the total collisional cross section for vibrational relaxation should be even larger. The possibility of increased total cross section arises from the probable contribution of near-resonant processes such as the following:

1. $\text{CO}_2 [10^00, 02^00]_{II} + \text{HBr} \rightarrow \text{CO}_2 [10^00, 02^00]_I + \text{HBr} + \Delta\text{KE}$
2. $\text{CO}_2 [10^00, 02^00]_{II} + \text{HBr} \rightarrow \text{CO}_2 02^20 + \text{HBr} + \Delta\text{KE}$
3. $\text{CO}_2 [10^00, 02^00]_{II} + \text{CO}_2 \rightarrow 2 \text{CO}_2 01^10 + \Delta\text{KE}$

At first glance the rapid relaxation of the upper 16 μ m laser level is not in itself deleterious. In principle, one could always overwhelm the relaxation by stimulating the $00^01-[10^00, 020]_{II}$ transition with a sufficiently intense pulse so as to achieve a transient gain. However, the initial V-V transfer from HBr is to all rotational sub-levels and thus for efficient extraction of all stored vibrational energy

it is necessary to wait for complete relaxation of the rotational manifold before the stimulating pulse can be turned off. As a result, relaxation of the upper $16\text{ }\mu\text{m}$ level must not be faster than relaxation of the rotational manifold or energy extraction will be inefficient. Earlier observations in a non-wavelength selective cavity suggested that this relaxation time, while fast, was still slower than rotational relaxation. By using a grating tuned cavity we have shown in a more direct manner that this is indeed the case.

Figure 1-2 shows the grating tuned cavity which was used for experiments. Note that because of the three Brewster windows and the diffraction grating the cavity was relatively lossy. With this cavity, it was found that a wide range of spectral lines could be selected for each choice of pump line. As an example, stimulating lines from P(8) to P(30) could be used to obtain $16\text{ }\mu\text{m}$ laser action on the P(19) transition. In addition, each P or R branch transition in the $9.6\text{ }\mu\text{m}$ band could be used to stimulate P, Q, or R branch transitions in the $16\text{ }\mu\text{m}$ laser band. When the cavity was tuned so that the resonant line and the stimulating line were connected, viz. P(19) and P(18), respectively, no dramatic increase in the strength of the $16\text{ }\mu\text{m}$ signal was seen.* These results demonstrate that rotational equilibration is complete before the upper $16\text{ }\mu\text{m}$ laser level is relaxed.

With this cavity, an attempt was made to stimulate with the $10.6\text{ }\mu\text{m}$ CO_2 transition and still observe $16\text{ }\mu\text{m}$ laser action. The results of this experiment would indicate whether equilibration of the population between the levels equi-energetic to the $[00^01, 02^00]_{\text{II}}$ level was the initial step in relaxing the $16\text{ }\mu\text{m}$ upper laser level. Despite the fact that, for this experiment, a higher reflectivity mirror was used in place of the 80% mirror shown in Fig. 1-2, $16\text{ }\mu\text{m}$ laser emission was not seen when stimulating with $10.6\text{ }\mu\text{m}$.

*This result is qualitative; more detailed measurements need be made.

Improvements in the OPL

There were two noteworthy improvements in the OPL. First, as described above, single line, grating tuned oscillation was obtained. While the 16 μm pulse energy was not measured systematically for the grating tuned laser, preliminary measurements indicate that it was approximately one-fourth of that measured with the multi-line cavity. Considering the losses in this cavity, this "rough" measurement indicates that the optimized energy will be comparable for single and multi-line operation.

The second major improvement was the attaining of 0.3 mJ from the OPL. This result was achieved with a particularly long OPL sample cell. The improvement most likely results from the relatively lower partial pressure of HBr gas which is sufficient to achieve complete absorption in such a long cell. Since the total pressure (mostly argon) was still as high as in a shorter cell, the ratio of rotational relaxation rate to vibrational rate increased as the cell length was increased. This accounts for the improvement in energy output. Note, that the laser efficiency is still about a factor of eight less than expected from theoretical considerations; thus further improvement can be expected.

Redesign of OPL System

A considerable amount of effort was expended on redesign of the entire OPL system. This effort was necessary to increase the reliability of the bromine handling components, and to increase the flexibility for varying various cavity configurations. The redesign has resulted in an improved HBr laser and associated cryogenic traps. In addition, the optical layout has been simplified and improved.

Conclusions

We summarize the major findings of this semiannual as follows:

1. Single-line laser action was observed from the rotational levels of interest.
2. A pulse energy of 0.3 mJ was obtained at 16 μm .
3. Rotational relaxation of the upper 16 μm laser level occurs before its vibrational relaxation in typical HBr-CO₂ OPL mixtures.

R. M. Osgood, Jr.

Figure Captions:

- 1-1 Energy level diagram showing the levels of CO₂ and HBr which are relevant to the 16 μm optically pumped laser.
- 1-2 Grating tuned cavity used for the 16 μm optically pumped laser.

Fig. 1-1

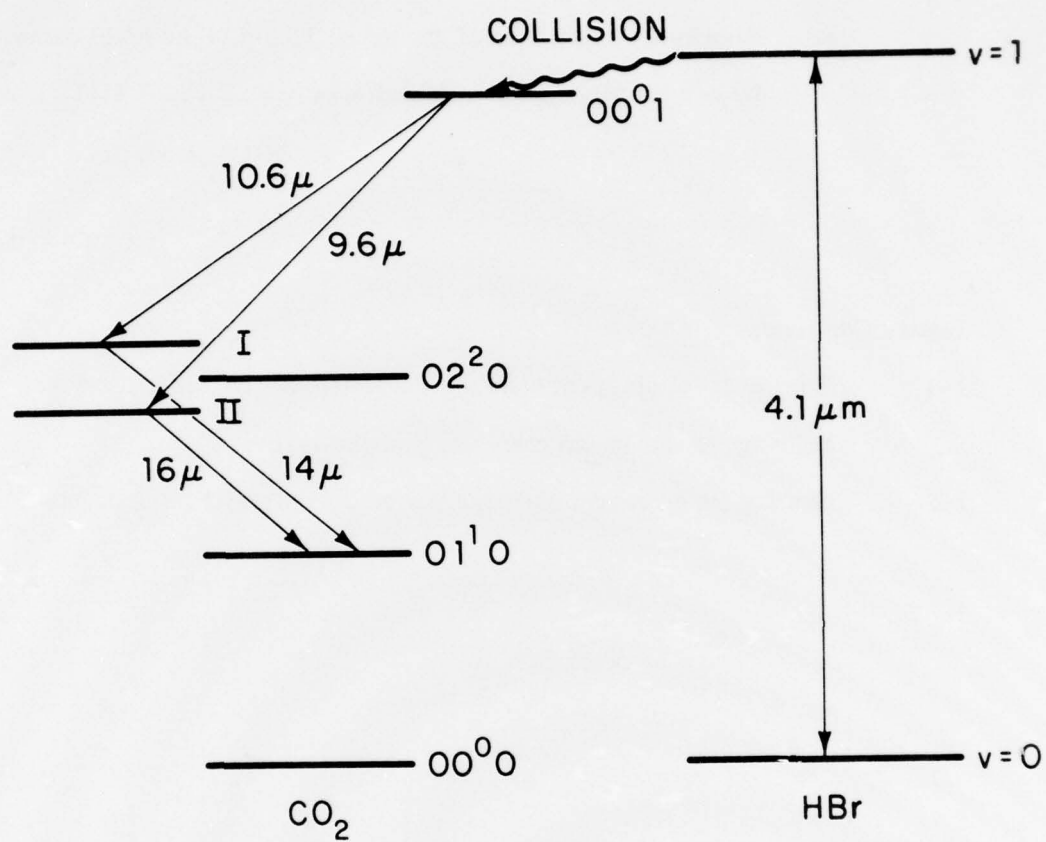
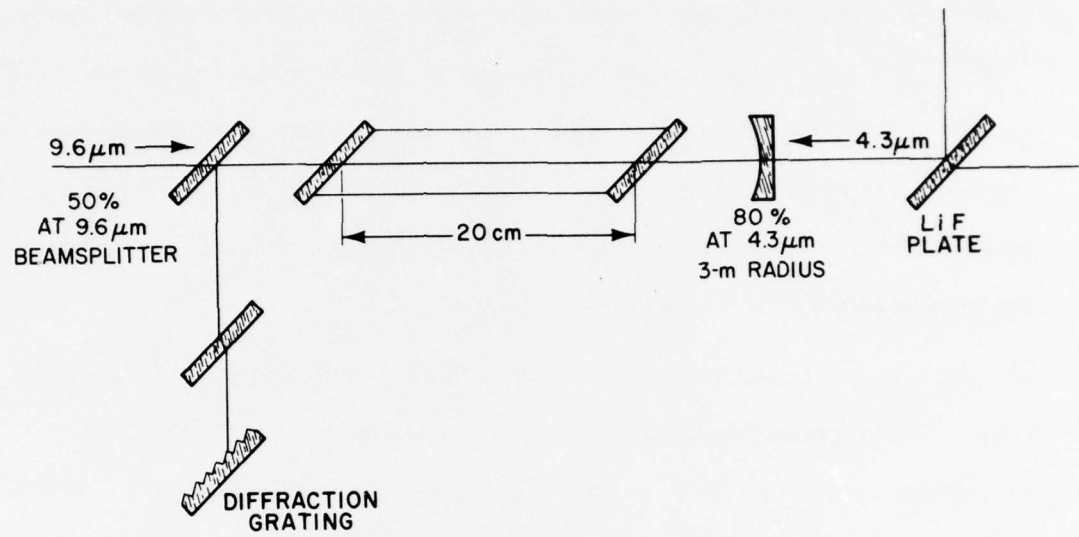


Fig. 1-2



2. OPTICALLY PUMPED 7.75 AND 8.62 μm LASER DEVELOPMENT

Measurements of the $^{16}\text{O}^{13}\text{C}^{32}\text{S}$ laser emission wavelengths are currently in progress. The preliminary results obtained using a 1 m Jarrell-Ash spectrometer are listed in Table 2-1. The measured threshold for the isotopic $^{16}\text{O}^{13}\text{C}^{32}\text{S}$ laser is about 4 to 5 times higher than the observed threshold for the normal isotope $^{16}\text{O}^{12}\text{C}^{32}\text{S}$ laser. Presently we do not know if this represents an intrinsic difference or if it is related to the purity of the gases. We have therefore ordered some $^{16}\text{O}^{13}\text{C}^{32}\text{S}$ from Prochem to make a comparison with the $^{16}\text{O}^{13}\text{C}^{32}\text{S}$ gas supplied by Los Alamos. In the present cavity configuration the measured threshold for the grating tuned $^{16}\text{O}^{13}\text{C}^{32}\text{S}$ laser is about 15 mJ.

We have obtained an output energy of 5.2 mJ from a directly pumped $^{16}\text{O}^{12}\text{C}^{32}\text{S}$ laser. The measured efficiency is 19 percent while the theoretical efficiency for unit quantum efficiency is 58 percent. We believe the slow deactivation rate of the 10^0 lower laser level limits the maximum efficiency to half unit quantum efficiency. The deactivation rate of the ν_1 mode is approximately $3.4 \times 10^3 \text{ sec}^{-1} \text{ Torr}^{-1}$ so that at a typical operating pressure of 10 Torr the deactivation time is 29 μsec . This is long compared to the 200 nsec duration of the OCS laser output pulse. Increasing the pressure above 10 Torr will not increase the efficiency since this also increases the deactivation of the upper laser level, whose rate is $4.7 \times 10^4 \text{ sec}^{-1} \text{ Torr}^{-1}$. We are investigating gases which might affect the deactivation rate of the lower laser level without changing the deactivation rate of the upper level significantly.

H. Kildal
T. F. Deutsch

Table 2-1

Preliminary Vacuum Wavenumber Measurements for the O¹³CS Laser

R-branch	P-branch
1159.77	1149.73
1160.18	1148.13*
1160.52	1147.67
1160.97	1146.41*
1161.29	1145.42
1162.00	1145.09*
1162.40	1144.26
1162.78	1143.83
1162.94*	1141.21
1163.63*	
1164.08	
1164.30	
1164.47	
1164.83*	
1167.35	
1168.13	

*Reported previously.

3. CALIBRATION OF $^{14}\text{C}^{16}\text{O}_2$ LASER LINES

Absolute frequency calibration of the $^{14}\text{C}^{16}\text{O}_2$ laser transitions is currently under way. The data for absolute frequency calibration are obtained with a two-channel, line-center stabilized CO_2 laser heterodyne frequency calibration system. Detailed description of the calibration system and procedure is given in Appendix 3-A.

The frequency stability and reproducibility of the entire calibration system was recently tested by measuring the time domain fractional frequency stability of the 2,697.86 MHz beat frequency between the $^{12}\text{C}^{16}\text{O}_2$ $00^0_1 - [10^0_0, 02^0_0]_I$ band P(20) and the $^{13}\text{C}^{18}\text{O}_2$ $00^0_1 - [10^0_0, 02^0_0]_I$ band R(24) laser transitions. Extensive measurements of the Allan Variance on the above beat frequency yielded a fractional frequency stability of $\sigma_y(\tau) \approx 6 \times 10^{-12} \tau^{-1/2}$, where τ is the observation time in seconds. The time domain stability measurements yielded the optimum operating parameters for the isotope calibration system. Further details and results are given in Appendix 3-B.

After a thorough checkout and optimization of the entire system we commenced with the precise calibration of the $^{14}\text{C}^{16}\text{O}_2$ laser transitions. This is much more time consuming than our previous measurements on CO_2 isotopes because no single CO_2 isotope laser overlaps more than one branch of the $^{14}\text{C}^{16}\text{O}_2$ spectrum, as indicated by Fig. 3-1. Thus we have to use three different CO_2 isotope lasers just to calibrate the three short wavelength branches of $^{14}\text{C}^{16}\text{O}_2$. The fourth branch covering the 12 μm region has to be obtained from heterodyne measurements of adjacent pairs of $^{14}\text{C}^{16}\text{O}_2$ lasing transitions with beat frequencies in the 50 to 70 GHz region.

At the present writing we have completed the measurements of about two dozen beat frequencies between the $^{14}\text{C}^{16}\text{O}_2$ $00^0_1 - [10^0_0, 02^0_0]_{11}$ band P and R transitions and adjacent $^{12}\text{C}^{16}\text{O}_2$ and $^{13}\text{C}^{18}\text{O}_2$ laser lines. In order to facilitate the $^{14}\text{C}^{16}\text{O}_2$ measurements we have also recalibrated the $^{13}\text{C}^{18}\text{O}_2$ lines with more than a 1000-fold improvement in accuracy.

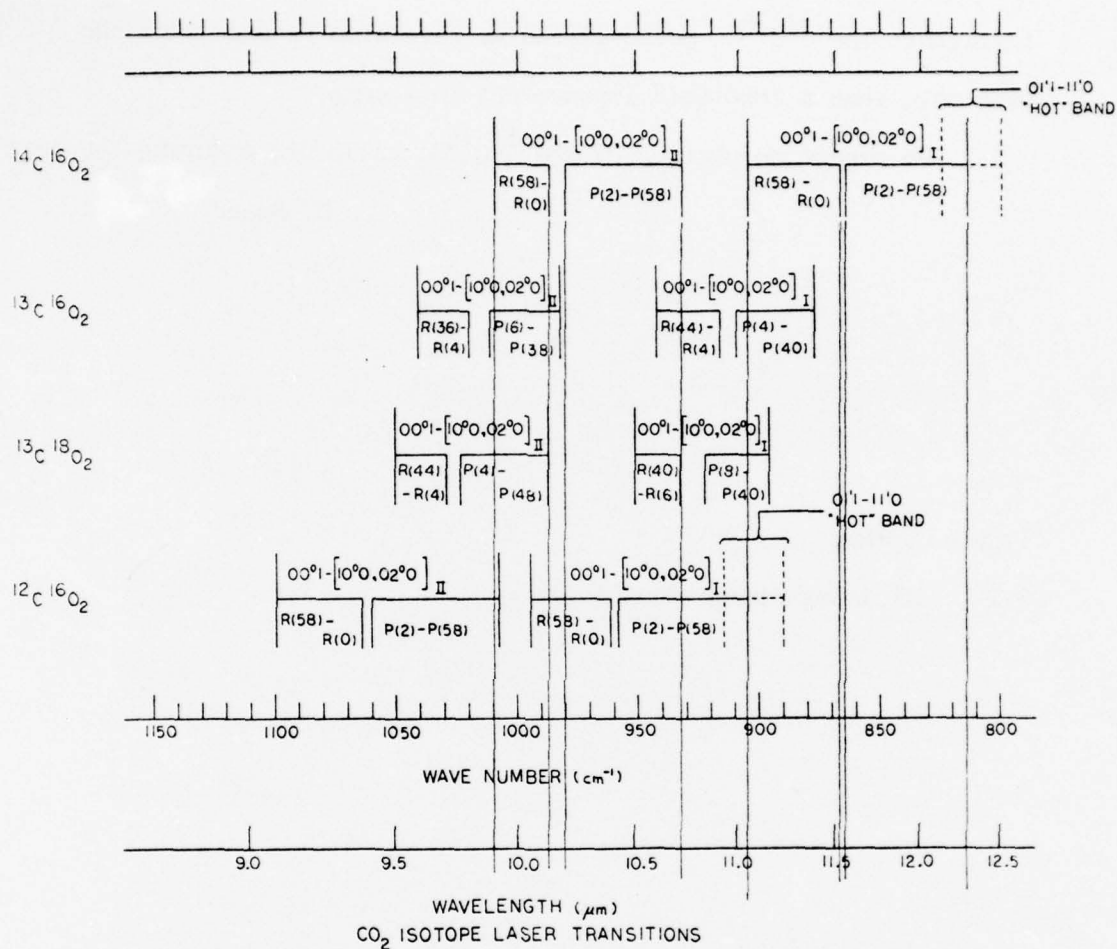
We expect completion of the $^{14}\text{C}^{16}\text{O}_2$ calibration during the next quarter.

C. Freed

Figure Caption:

3-1 CO_2 isotope laser transitions.

Fig. 3-1



Absolute Frequency Calibration of the CO₂
Isotope Lasers Transitions*

by

C. Freed and R. G. O'Donnell

M. I. T. Lincoln Laboratory
Lexington, Massachusetts

and

A. H. M. Ross

U.C.L.A. Dept. of Physics
Los Angeles, California

Presented at

The 1976 Conference on Precision Electromagnetic Measurements

held

June 28 - July 1, 1976

at

Boulder, Colorado

PREPRINT

To be published in the December 1976 issue of IEEE Trans. Instrum. Meas.

*This work was sponsored by the Advanced Research Projects Agency of the Department of Defense and in part by U. S. Energy Research and Development Administration.

Absolute Frequency Calibration of the
CO₂ Isotope Laser Transitions*

Abstract

The frequencies of rare CO₂ isotope lasers are measured by comparison with ¹²C¹⁶O₂ reference lines and with each other. Improved heterodyne techniques are used to generate difference frequencies in a liquid-nitrogen-cooled HgCdTe varactor photodiode. Microwave frequency counter measurements of the difference frequencies are then used to calculate the band centers, rotational constants and transition frequencies with an estimated accuracy of less than a few kHz. Selected applications of CO₂ isotope lasers in precision heterodyne calibration, spectroscopy, microwave and IR synthesis are described.

* This work was sponsored by the Advanced Research Projects Agency of the Department of Defense and in part by U. S. Energy Research and Development Administration.

Absolute Frequency Calibration of the CO₂ Isotope Laser Transitions*

Introduction

This paper will concentrate on new results relating to CO₂ isotope lasers.⁽¹⁾ At the June 1973 Laser Spectroscopy Conference in Vail, Colorado, we reported on the determination of transition frequencies, band centers and rotational constants of ¹²C¹⁸O₂, ¹³C¹⁶O₂, and ¹³C¹⁸O₂ isotope lasers^(2,3) with accuracies of about 3 MHz. At least a 1000-fold improvement in accuracy has been achieved with the experimental apparatus currently in use. Also, hundreds of new lasing transitions have been observed in ¹⁶O¹²C¹⁸O, ¹⁶O¹³C¹⁸O, and ¹⁴C¹⁶O₂, and measurements of ¹⁴C¹⁸O₂ and ¹⁶O¹⁴C¹⁸O lasers will be carried out in the near future.

Current Experiments

Optical heterodyne techniques^(2,3,4,5) are used to generate beat frequencies between two lasers either filled with different CO₂ isotopes, or if the same isotope is used the difference frequencies between adjacent rotational transitions are measured. The band centers are determined by two heterodyne comparisons with the ¹²C¹⁶O₂ lines measured by Evenson et al.⁽⁶⁾ The rotational constants are computed by fitting the measured difference frequencies in a least squares sense to the expansion of the line frequencies

$$\begin{aligned} f = & f_0 + B_u [J'(J'+1) - J(J+1)] - (B_l - B_u) J(J+1) \\ & - D_u [J'^2(J'+1)^2 - J^2(J+1)^2] + (D_l - D_u) J^2(J+1)^2 \\ & + H_u [J'^3(J'+1)^3 - J^3(J+1)^3] - (H_l - H_u) J^3(J+1)^3 \\ & - L_u [\dots \end{aligned} \tag{1}$$

where $J' = J-1$ for a P(J) line and $J' = J+1$ for an R(J) line. Figure 1 shows a block diagram of the experimental apparatus.

The experimental procedure is similar in principle to the one previously described;^(2,3) therefore this paper will emphasize the improvements achieved and avoid repetition of every detail.

Refinements in our standard grating controlled laser design^(2,3,7) resulted in greatly improved laser output with tap-water cooling. About 150 transitions lasing in the TEM_{00q} mode could be obtained with a pure CO₂ isotope fill, including many from the 01¹1 - 11¹0 "hot band". Several hundred lasing transitions were available from a single laser filled with mixed isotopes.

The 1000-fold improvement in the accuracy of frequency measurements was primarily due to active long-term stabilization of the lasers to the natural line centers of low pressure, room temperature, CO₂ absorption cells external to the lasers. In previous papers with A. Javan we have shown^(8,9) that CO₂ lasers can be frequency-stabilized in any lasing transition by using the standing-wave saturation resonances in a low pressure, room temperature pure CO₂ absorber via the intensity changes observed in the entire collisionally coupled spontaneous emission band at 4.3 μ m. It was also demonstrated that the frequency shift due to changes in pressure is very small in CO₂, typically much less than 100 Hz/mTorr.

In the experimental setup shown in Fig. 1, vastly improved CO₂ stabilization cells external to the lasers are used.⁽¹⁰⁾ In the new design, the low pressure gas cell, the LN₂-cooled radiation collector, and the IR detector are all integral parts of one evacuated housing assembly which also minimizes signal absorption by windows and eliminates all other sources of absorption. Because of the vacuum enclosure, diffusion of other gases into the low-pressure gas reference cell is

almost completely eliminated; therefore, the time period available to use the reference gas cell has greatly increased and considerably less time has to be wasted on repumping and refilling procedures. Also, one LN_2 fill will last at least 18 hours. In addition to greatly improved reliability and maintenance we have also obtained⁽¹⁰⁾ at least two orders of magnitude improvement of the signal-to-noise ratio in measuring the $4.3 \mu\text{m}$ fluorescence.

The improvements in laser stability also necessitated the use of highly stabilized microwave oscillators and frequency counters to measure both the intermediate and the local oscillator frequencies. The frequency counts were directly fed into a computer for further processing of the data.

No description of our experimental setup can be complete without specially mentioning the remarkable performance achieved with the improved, high speed, high quantum efficiency HgCdTe photodiodes developed by D. L. Spears at Lincoln Laboratory. We achieve mixing of the microwave local oscillator, or its harmonics, with the CO_2 laser beats directly in these HgCdTe photodiodes. The generation of harmonics and the mixing of the microwave signals closely correspond to varactor diode behavior.⁽¹¹⁾ Figure 2 illustrates a typical microwave frequency beat signal obtained by varactor harmonic mixing and frequency down-conversion in such a photodiode. Figure 2 shows a 52 dB signal-to-noise ratio with a 10 kHz noise bandwidth for the 24,410.301 MHz beat frequency of the $^{16}\text{O}^{12}\text{C}^{18}\text{O} \ 00^0_1 - [10^0_0, 02^0_0]_I$ band P(12) and the $^{12}\text{C}^{16}\text{O}_2 \ 00^0_1 - [10^0_0, 02^0_0]_I$ band P(6) transitions; this represents a 16 dB increase in signal-to-noise ratio when compared to our previously published results.^(2,3) Greater detection sensitivity was due in part to improvements in detector technology and in part to special, low microwave loss dewar and signal-duplexer design. The two detectors presently in use have been installed well over two years ago and both can detect

the up to 60 GHz (2 cm^{-1}) beat frequencies of adjacent CO_2 rotational transitions with over 30 dB signal-to-noise ratio.

Table I shows a set of 20 beat frequencies measured between the indicated $^{16}\text{O}^{12}\text{C}^{18}\text{O}$ isotope transitions and adjacent $^{12}\text{C}^{16}\text{O}_2$ laser lines used as reference. The measured difference frequencies were fitted in a least squares sense to the expansion of the line frequencies shown previously in Eq. 1. The $^{12}\text{C}^{16}\text{O}_2$ reference frequencies were computed from the constants recently published by Petersen⁽⁵⁾ and his coworkers at the N.B.S. in Boulder.

Table II shows the band centers and rotational constants of $^{16}\text{O}^{12}\text{C}^{18}\text{O}$ determined from the twenty beat frequencies listed in Table I. The results in Tables I and II show more than 10^4 improvement over the data previously available for this isotope. We expect another order of magnitude improvement because the data of Table I were taken prior to installation of the improved laser stabilization equipment.⁽¹⁰⁾

Hundreds of laser lines have been observed in $^{16}\text{O}^{12}\text{C}^{18}\text{O}$ and in $^{16}\text{O}^{13}\text{C}^{18}\text{O}$ isotopes since both even and odd rotational transitions are allowed for a linear molecule in which one of the atoms is replaced by an isotopic substitute. Our current emphasis, however, lies in the determination of the $^{14}\text{CO}_2$ laser transitions because of the rich spectrum they provide in the vicinity of $12 \mu\text{m}$. Some of the $01^1_1 - 11^1_0$ "hot band" lines we observe are near $12.4 \mu\text{m}$ in $^{14}\text{C}^{16}\text{O}_2$ lasers. Figure 3 illustrates the relative positions of lasing transitions in $^{14}\text{C}^{16}\text{O}_2$, $^{16}\text{O}^{13}\text{C}^{18}\text{O}$, $^{16}\text{O}^{12}\text{C}^{18}\text{O}$ and $^{12}\text{C}^{16}\text{O}_2$ isotopes. We previously published^(2,3) a similar chart for the $^{13}\text{C}^{18}\text{O}_2$, $^{13}\text{C}^{16}\text{O}_2$ and $^{12}\text{C}^{18}\text{O}_2$ isotopes.

It is thus clear that the spectral purity, frequency stability and resettability together with the availability of well over a thousand lasing transitions uniquely endow the CO_2 system for either direct use in high resolution spectroscopy, or as a secondary frequency standard in heterodyne spectroscopy with tunable lasers, or in precision IR synthesis which involves frequency mixing. Examples of such uses will be given in the remaining part of this paper.

CO_2 Laser Applications in IR Spectroscopy and Synthesis

The examples described in this section have been selected because of some personal interest or involvement of the author and are not meant to be all inclusive. By comparison with selected, doubled CO_2 transitions⁽¹²⁾ the entire CO laser spectrum may be also utilized as a secondary frequency standard in the 4.9 to 7.5 μm portion of the infrared spectrum. With the sole exception of the saturation resonance stabilization technique using the 4.3 μm spontaneous emission, all other aspects of this paper can be easily extended to the molecular CO laser system. Stable, sealed-off CO laser operation has been previously demonstrated.⁽¹³⁾ The Lamb-dip in CO lasers⁽¹⁴⁾ can be used to set the laser transitions well within 1 MHz of line center. The HgCdTe varactor photodiodes are just as useful at CO wavelengths. Indeed, microwave frequency beats between CO laser transitions equivalent to the one shown in Fig. 2 have been previously described.^(2,12,15,16)

Figure 4 illustrates probably the most precise measurement method available to date in the calibration of absorption spectra. In the experimental arrangement of Fig. 4, the outputs of a tunable diode laser and a $^{14}\text{C}^{16}\text{O}_2$ laser are combined by a beam splitter. One part of the combined radiation is heterodyned on a fast HgCdTe varactor photodiode,⁽¹¹⁾ and the beatnote displayed and measured

by a microwave spectrum analyzer (or counter). The other part of the combined laser radiation is used to probe an absorption cell, which in this particular experiment was filled with NH_3 at a pressure of 5 TORR.

Figure 5 shows a heterodyne beat frequency of 6,775 MHz between the $^{14}\text{C}^{16}\text{O}_2$ laser and the diode laser tuned to one of the NH_3 absorption lines near 12.1 μm . With the CO_2 laser stabilized to its line center and the diode laser locked to the absorption line to be measured, heterodyne calibration can provide an accuracy not presently available by any other method.

At Kitt Peak National Observatory, in a whole series of beautiful experiments, heterodyne detection was used to measure CO_2 emission lines in the atmospheres of Venus and Mars. The observed frequencies have been combined with a knowledge of the CO_2 transition rest frequencies and the center of mass velocity of the planet to determine the line-of-sight wind velocities in the upper atmosphere of Venus.^(18,19)

In heterodyne experiments with CO_2 lasers it is often advantageous to use a local oscillator with a precisely known offset frequency. For instance knowledge of the 910.365 MHz beat frequency between the $^{13}\text{C}^{16}\text{O}_2$ $[10^0_0, 02^0_0]_1$ P(16) and the $^{12}\text{C}^{16}\text{O}_2$ $01^1_1 - 11^1_0$ band P(31) transitions provided a convenient choice in the observation of hot band emission lines in the atmosphere of Mars.⁽¹⁹⁾

The computerized setup shown in Fig. 1 gives great flexibility in the processing and use of accumulated experimental results. For example, Table III shows the beat frequencies from 0 to 2000 MHz, computed and sorted for the $^{12}\text{C}^{16}\text{O}_2$ and $^{16}\text{O}^{12}\text{C}^{18}\text{O}$ isotopes.

Microwave (or lower) frequency generation may be achieved with a single laser filled with a mixture of CO_2 isotopes. The spectral purity and long term stability of the (self-) beatnotes obtained in this way may only be compared to

stabilized oscillators of the highest quality. Figure 6 shows the spectrum analyzer display of the 3165 MHz self-beat frequency of the $^{14}\text{C}^{16}\text{O}_2$ $00^0_1 - [10^0_0, 02^0_0]_{II}$ P(10) and the $^{12}\text{C}^{16}\text{O}_2$ $00^0_1 - [10^0_0, 02^0_0]_I$ R(18) transitions. The spectral purity of such self-beats is explained by the fact that the fractional frequency stability at the microwave beat frequency will be identical to the stability of the laser frequency itself. Short-term stabilities of 10^{-11} to 10^{-13} are routinely achieved with well designed and acoustically shielded CO_2 lasers in a normal laboratory environment.⁽²⁰⁾ Microwave oscillators must utilize superconducting cavities to achieve the high Q factors necessary for equivalent stability.

Table IV illustrates IR synthesis at 16 μm , in which the computer was given the task to find all possible CO_2 isotope line combinations for which the difference frequency between frequency doubled $^{14}\text{C}^{16}\text{O}_2$ transitions and any other CO_2 transition will fall within $625.0 \pm 0.1 \text{ cm}^{-1}$. (It should be noted, however, that Table IV was computed from our preliminary spectrometer measurements on $^{14}\text{C}^{16}\text{O}_2$ and should not be considered final and accurate, but rather as an example of methodology.)

Conclusions

Rare CO_2 isotopes can provide a many-fold expansion of the already highly useful spectral range of CO_2 lasers. In terms of number of lasing transitions, power output, gain, stability, and sealed-off cw operation characteristics, rare isotope lasers are generally similar to the commonly used $^{12}\text{C}^{16}\text{O}_2$ lasers. Since sealed-off CO_2 laser operating life times of over 10,000 hours have been reported

by a number of laboratories, the additional cost of a few Torr-liters of isotope required for a properly designed laser is not significant.

Even the few examples given in this paper make it quite clear that the spectral purity, frequency stability and resettability together with the availability of well over a thousand lasing transitions uniquely endow the CO_2 system for either direct use in high resolution spectroscopy or as a secondary frequency standard in heterodyne spectroscopy with tunable lasers, or in precision IR synthesis which involves frequency mixing.

A systematic and precise evaluation of the band centers, rotational constants, and lasing transition frequencies of the CO_2 isotopes is under way. These data will also be of great value in evaluating the potential function under the influence of which the nuclei are moving.

Acknowledgements

The author is deeply appreciative to K. Nill for collaboration in heterodyne spectroscopy with a tunable diode laser, and to D. L. Spears for providing the fast HgCdTe varactor-photodiodes.

References

1. For a review of previous work on CO₂ isotope lasers see the introduction in Reference 2 or 3.
2. C. Freed, D. L. Spears, R. G. O'Donnell, and A. H. M. Ross, "Precision Heterodyne Calibration," Proc. of the Laser Spectroscopy Conference, June 25-29, 1973, Vail, Colorado. Also in Laser Spectroscopy, pp. 171-191, Plenum Press, 1975, (R. A. Brewer and A. Mooradian, Editors).
3. C. Freed, A. H. M. Ross and R. G. O'Donnell, "Determination of Laser Line Frequencies and Vibrational-Rotational Constants of the ¹²C¹⁸O₂, ¹³C¹⁶O₂, and ¹³C¹⁸O₂ Isotopes from Measurements of CW Beat Frequencies with Fast HgCdTe Photodiodes and Microwave Frequency Counters," J. Molecular Spectrosc., vol. 49, p. 439, 1974.
4. T. J. Bridges and T. Y. Chang, "Accurate Rotational Constants of ¹²C¹⁶O₂ from Measurements of CW Beats in Bulk GaAs between CO₂ Vibrational-Rotational Laser Lines," Phys. Rev. Lett., vol. 22, pp. 811-814, April 21, 1969.
5. F. R. Petersen, D. G. McDonald, J. D. Cupp, and B. L. Danielson, "Accurate Rotational Constants, Frequencies, and Wavelengths from ¹²C¹⁶O₂ Lasers Stabilized by Saturated Absorption," Proc. of the Laser Spectroscopy Conference, June 25-29, 1973, Vail, Colorado.
6. K. M. Evenson, J. S. Wells, F. R. Petersen, B. L. Danielson and G. W. Day, "Accurate Frequencies of Molecular Transitions used in Laser Stabilization: the 3.39-μm transition in CH₄ and the 9.33- and 10.18-μm transitions in CO₂," Appl. Phys. Lett. vol. 22, pp. 192-195, February 15, 1973.
7. C. Freed, "Designs and Experiments Relating to Stable Lasers," Proceedings of the Frequency Standards and Metrology Seminar, University Laval, Quebec, Canada, pp. 226-261, September 1, 1971.
8. C. Freed and A. Javan, "Standing-Wave Saturation Resonances in the 10.6 μm Transitions Observed in a Low-Pressure Room-Temperature Absorber Gas," Appl. Phys. Lett. vol. 16, pp. 53-56, July 15, 1970.
9. C. Freed and A. Javan, "Standing-Wave Saturation Resonances in Room Temperature CO₂ 10.6 μm Absorption Lines," Paper 4.4 presented at the 1970 Sixth International Quant. Elect. Conference, September 1970, Kyoto, Japan.

10. C. Freed, "Frequency Stabilization of CO₂ Lasers," Proc. of the 29th Annual Symposium on Frequency Control, May 28-30, 1975, Atlantic City, N.J., pp. 330-337.
11. D. L. Spears and C. Freed, "HgCdTe Varactor Photodiode Detection of CW CO₂ Laser Beats Beyond 60 GHz," Appl. Phys. Lett., vol. 23, p. 445, 1973.
12. R. S. Eng, H. Kildal, J. C. Mikkelsen and D. L. Spears, "Determination of Absolute Frequencies of ¹²C¹⁶O and ¹³C¹⁶O Laser Lines." Appl. Phys. Lett., vol. 24, pp. 231-233, 1974.
13. C. Freed, "Sealed-off Operation of Stable CO Lasers," Appl. Phys. Lett., vol. 18, pp. 458-461, 1974.
14. C. Freed and H. A. Haus, "Lamb Dip in CO lasers," IEEE J. Quantum Electron., vol. QE-9, pp. 219-226, 1973.
15. H. Kildal, R. S. Eng, and A. H. M. Ross, "Heterodyne Measurements of ¹²C¹⁶O Laser Frequencies and improved Dunham Coefficients," J. Molecular Spectrosc., vol. 53, pp. 479-488, 1974.
16. A. H. M. Ross, R. S. Eng, and H. Kildal, "Heterodyne Measurements of ¹²C¹⁸O, and ¹³C¹⁸O Laser Frequencies; Mass Dependence of Dunham Coefficients," Optics Communications, vol. 12, pp. 433-438, December 1974.
17. C. Freed and K. Nill, "12.2 μm Wavelength Calibration," Semiannual Report in Support of the Jumper Program for Laser Isotope Separation, pp. 70-78, Dec., 1975.
18. A. L. Betz, M. A. Johnson, R. A. McLaren, and E. C. Sutton, "Heterodyne Detection of CO₂ Emission Lines and Wind Velocities in the Atmosphere of Venus," to be published.
19. A. L. Betz, M. A. Johnson, R. A. McLaren, and E. C. Sutton, "Infrared Heterodyne Spectroscopy of CO₂ in the Atmosphere of Mars," to be published.
20. C. Freed, "Design and Short-Term Stability of Single-Frequency CO₂ Lasers," IEEE J. Quant Electron., vol. QE-4, p. 404, 1968.

Table I. Difference frequencies measured between $^{16}\text{O}^{12}\text{C}^{18}\text{O}$ and $^{12}\text{C}^{16}\text{O}_2$ lasing transitions.

Table II. Band centers and rotational constants (in MHz) for $^{16}\text{O}^{12}\text{C}^{18}\text{O}$.

Table III. Beat frequency generation in the 0 to 2000 MHz range by synthesis of $^{12}\text{C}^{16}\text{O}_2$ and $^{16}\text{O}^{12}\text{C}^{18}\text{O}$ isotope laser transitions.

Table IV. Computerized IR synthesis at $16\text{ }\mu\text{m}$ to find all possible CO_2 isotope line combinations for which the difference frequency between frequency doubled $^{14}\text{C}^{16}\text{O}_2$ and any other CO_2 transition will fall within $625.0 \pm 0.1\text{ cm}^{-1}$.

Figure Captions

Fig. 1. Experimental setup used to determine the CO₂ isotope laser frequencies.

Fig. 2. 24,410.301 MHz beat frequency of the ¹⁶O¹²C¹⁸O laser 00⁰1 - [10⁰0, 02⁰0]_I band P(12) and the ¹²C¹⁶O₂ laser 00⁰1 - [10⁰0, 02⁰0]_I band P(6) transitions.
Power levels into photodiode:

¹²C¹⁶O₂ LASER : 0.42 mw

¹⁶O¹²C¹⁸O LASER : 0.48 mw

Noise bandwidth : 10 kHz

Second harmonic of microwave L.O. is used.

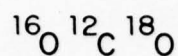
Fig. 3. Comparison of the frequency domain of rare CO₂ isotope lasers with ¹²C¹⁶O₂.

Fig. 4. Experimental setup used to calibrate NH₃ absorption lines at 12.1 μm.

Fig. 5. Spectrum analyzer display of a 6,775 MHz beat frequency between a ¹⁴C¹⁶O₂ laser transition and a tunable diode laser probe held to one of the NH₃ absorption lines near 12.1 μm.

Fig. 6. Spectrum analyzer display of 3,165 MHz beat frequency of the ¹⁴C¹⁶O₂ 00⁰1 - [10⁰0, 02⁰0]_{II} band P(10) and the ¹²C¹⁶O₂ 00⁰1 - [10⁰0, 02⁰0]_I band R(18) transitions.

TABLE I

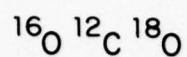


Isotope Line	Reference Line	Measured f(I) - f(R) (MHz)	Meas.-Calc. (kHz)
I P(36)	I P(30)	23093.472233	0.319
I F(30)	I P(24)	24056.453370	-4.910
I P(28)	I P(22)	24281.326590	11.685
I F(26)	I P(20)	24458.722416	-9.601
I P(12)	I P(6)	24410.301202	-0.837
I F(20)	I R(26)	16293.464805	7.006
I R(22)	I R(28)	15492.423925	-6.201
I F(24)	I R(30)	14661.591163	2.163
I R(26)	I R(32)	13801.985927	-3.534
I F(28)	I R(34)	12914.731880	4.148
I R(30)	I R(36)	12000.945390	1.706
I F(32)	I R(38)	11061.821500	-1.943
II P(24)	II P(12)	-13727.654393	-0.455
II F(23)	II P(12)	12200.062893	-1.532
II P(21)	II P(10)	12550.189553	9.409
II F(20)	II P(8)	-12234.574563	-1.442
II P(19)	II P(8)	13033.172350	-2.832
II R(13)	II R(26)	3066.690077	-3.714
II R(15)	II R(28)	6484.301600	7.754
II R(19)	II R(32)	13634.173280	-7.188

Standard deviation= 8.226 kHz

DIFFERENCE FREQUENCIES MEASURED
BETWEEN $^{16}\text{O} \ ^{12}\text{C} \ ^{18}\text{O}$ AND $^{12}\text{C} \ ^{16}\text{O}_2$
LASING TRANSITIONS

TABLE II



NU I	=	28968012.096378	±	2.425E-02
NU II	=	32158350.546717	±	9.860E-02
B 001	=	10951.024273309	±	3.979E-04
B -B I 001	=	96.700681735529	±	1.406E-04
B -B II 001	=	84.981411491412	±	8.990E-04
D 001	=	3.5527097121690E-03	±	5.490E-07
D -D I 001	=	-4.8755934078738E-04	±	2.277E-07
D -D II 001	=	5.4516002699856E-04	±	2.481E-06
H 001	=	9.7056436467953E-10	±	2.468E-10
H -H I 001	=	2.2601804334360E-09	±	1.079E-10
H -H II 001	=	5.1398380543550E-09	±	2.109E-09

BAND CENTERS AND ROTATIONAL CONSTANTS
IN MHz FOR $^{16}\text{O}^{12}\text{C}^{18}\text{O}$

TABLE III

$\Delta\nu$ (MHz)	$= \pm n \times \nu_{^{12}\text{C}^{16}\text{O}_2}$		$\pm n \times \nu_{^{16}\text{O}^{12}\text{C}^{18}\text{O}}$	
3.590500	=	1 * 16012C160	(0001,1000	P (6)
27.790000	=	1 * 16012C160	(0001,0200	R (8)
68.344400	=	-1 * 16012C160	(0001,1070	R (14)
144.304800	=	1 * 16012C160	(0001,1000	R (16)
197.785900	=	-1 * 16012C160	(0001,1000	P (4)
245.483700	=	-1 * 16012C160	(0001,1070	R (12)
248.712600	=	1 * 16012C160	(0001,1000	P (8)
262.406100	=	1 * 16012C160	(0001,0270	R (24)
356.102700	=	-1 * 16012C160	(0001,1000	P (2)
386.221600	=	-1 * 16012C160	(0001,1000	R (10)
391.546300	=	1 * 16012C160	(0001,1000	R (18)
489.692100	=	-1 * 16012C160	(0001,1000	R (8)
514.390200	=	-1 * 16012C160	(0001,1000	R (0)
538.247100	=	1 * 16012C160	(0001,1000	P (10)
550.550800	=	1 * 16012C160	(0001,1000	R (60)
568.188400	=	-1 * 16012C160	(0001,1000	R (2)
573.327800	=	-1 * 16012C160	(0001,1070	R (58)
581.483900	=	-1 * 16012C160	(0001,1000	R (4)
672.434700	=	1 * 16012C160	(0001,1000	R (20)
872.840600	=	1 * 16012C160	(0001,1000	P (12)
985.995100	=	1 * 16012C160	(0001,1000	P (22)
1163.742900	=	1 * 16012C160	(0001,0200	R (34)
1253.120000	=	1 * 16012C160	(0001,1000	P (14)
1331.221500	=	1 * 16012C160	(0001,1000	R (24)
1369.368300	=	1 * 16012C160	(0001,0200	R (60)
1526.544100	=	1 * 16012C160	(0001,0270	R (42)
1532.085300	=	-1 * 16012C160	(0001,0270	R (50)
1679.691900	=	1 * 16012C160	(0001,1000	P (16)
1680.857900	=	1 * 16012C160	(0001,1000	R (62)
1688.788900	=	-1 * 16012C160	(0001,1000	R (56)
1707.075200	=	1 * 16012C160	(0001,1000	R (26)
1944.147600	=	1 * 16012C160	(0001,0200	R (6)
2011.583500	=	-1 * 16012C160	(0001,0200	R (10)
2034.739500	=	-1 * 16012C160	(0001,0200	R (56)
2112.482400	=	1 * 16012C160	(0001,1000	R (28)
2153.141800	=	1 * 16012C160	(0001,1000	P (18)
2546.332500	=	1 * 16012C160	(0001,1000	R (30)
2674.033500	=	1 * 16012C160	(0001,1000	P (20)
2793.931300	=	-1 * 16012C160	(0001,1000	R (54)
2815.512100	=	1 * 16012C160	(0001,1000	R (64)
2913.889200	=	-1 * 16012C160	(0001,0200	R (36)
			-1 * 16012C180	(0001,1000) P (13)
			-1 * 16012C180	(0001,0200) P (3)
			1 * 16012C180	(0001,1000) R (7)
			-1 * 16012C180	(0001,1070) R (9)
			1 * 16012C180	(0001,1000) P (11)
			1 * 16012C180	(0001,1000) R (5)
			-1 * 16012C180	(0001,1000) P (15)
			-1 * 16012C180	(0001,0200) R (11)
			1 * 16012C180	(0001,1000) P (9)
			1 * 16012C180	(0001,1000) R (3)
			-1 * 16012C180	(0001,1000) R (11)
			1 * 16012C180	(0001,1000) R (1)
			1 * 16012C180	(0001,1000) P (6)
			-1 * 16012C180	(0001,1000) P (17)
			-1 * 16012C180	(0001,1000) R (54)
			1 * 16012C180	(0001,1000) P (4)
			1 * 16012C180	(0001,1000) R (52)
			1 * 16012C180	(0001,1000) P (2)
			-1 * 16012C180	(0001,1000) R (13)
			-1 * 16012C180	(0001,1000) P (19)
			-1 * 16012C180	(0001,1000) R (15)
			-1 * 16012C180	(0001,0200) R (20)
			-1 * 16012C180	(0001,1000) P (21)
			-1 * 16012C180	(0001,1000) R (17)
			-1 * 16012C180	(0001,0200) R (42)
			-1 * 16012C180	(0001,0200) R (27)
			1 * 16012C180	(0001,0200) R (34)
			-1 * 16012C180	(0001,1000) P (23)
			-1 * 16012C180	(0001,1000) R (56)
			1 * 16012C180	(0001,1000) R (50)
			-1 * 16012C180	(0001,1000) R (19)
			-1 * 16012C180	(0001,0200) P (5)
			1 * 16012C180	(0001,0200) P (1)
			1 * 16012C180	(0001,0200) R (39)
			-1 * 16012C180	(0001,1000) R (21)
			-1 * 16012C180	(0001,1000) P (25)
			-1 * 16012C180	(0001,1000) R (23)
			-1 * 16012C180	(0001,1000) P (27)
			1 * 16012C180	(0001,1000) R (48)
			-1 * 16012C180	(0001,1000) R (58)
			1 * 16012C180	(0001,0200) R (22)

BEAT FREQUENCY GENERATION IN THE 0-2000 MHz RANGE
 BY SYNTHESIS OF $^{12}\text{C}^{16}\text{O}_2$ AND $^{16}\text{O}^{12}\text{C}^{18}\text{O}$ ISOTOPE
 LASER TRANSITIONS

TABLE IV

$\nu_S(\text{cm}^{-1}) = 2 \times \nu_{14}\text{C}^{16}\text{O}_2$			$-1 \times \nu_{\text{CO}_2}$
624.901199 =	2 * 16014C160	(0001,1000 P (62)	-1 * 18012C180 (0001,1000) R (56)
624.901502 =	2 * 16014C160	(0001,1000 P (8)	-1 * 18012C180 (0001,0200) R (16)
624.920791 =	2 * 16014C160	(0001,1000 P (58)	-1 * 16013C180 (0001,0200) P (22)
624.923799 =	2 * 16014C160	(0001,1000 P (44)	-1 * 16013C160 (0001,0200) R (18)
624.949936 =	2 * 16014C160	(0001,1000 P (34)	-1 * 16013C180 (0001,0200) R (47)
624.956395 =	2 * 16014C160	(0001,1000 P (34)	-1 * 18013C180 (0001,0200) P (38)
624.960880 =	2 * 16014C160	(0001,1000 P (22)	-1 * 16012C180 (0001,0200) P (2)
624.965292 =	2 * 16014C160	(0001,1000 P (42)	-1 * 16012C180 (0001,0200) P (44)
624.968260 =	2 * 16014C160	(0001,1000 P (32)	-1 * 16012C180 (0001,0200) P (24)
624.976181 =	2 * 16014C160	(0001,1000 P (20)	-1 * 16012C160 (0001,0200) R (14)
624.977011 =	2 * 16014C160	(0001,1000 P (6)	-1 * 16012C180 (0001,0200) R (40)
624.982866 =	2 * 16014C160	(0001,1000 P (30)	-1 * 16013C180 (0001,0200) R (64)
624.999227 =	2 * 16014C160	(0001,1000 R (0)	-1 * 18012C180 (0001,0200) R (42)
625.000768 =	2 * 16014C160	(0001,1000 P (18)	-1 * 18012C180 (0001,0200) P (8)
625.013005 =	2 * 16014C160	(0001,1000 P (32)	-1 * 16013C180 (0001,0200) R (55)
625.019624 =	2 * 16014C160	(0001,1000 P (50)	-1 * 16012C180 (0001,0200) P (59)
625.024011 =	2 * 16014C160	(0001,1000 P (42)	-1 * 16013C160 (0001,0200) R (24)
625.032306 =	2 * 16014C160	(0001,1000 P (26)	-1 * 18012C180 (0001,0200) P (26)
625.035214 =	2 * 16014C160	(0001,1000 P (2)	-1 * 16012C180 (0001,0200) R (54)
625.046729 =	2 * 16014C160	(0001,1000 P (28)	-1 * 16012C160 (0001,0200) P (4)
625.051687 =	2 * 16014C160	(0001,1000 P (46)	-1 * 16013C160 (0001,0200) R (12)
625.065110 =	2 * 16014C160	(0001,1000 P (12)	-1 * 16012C180 (0001,0200) R (22)
625.077193 =	2 * 16014C160	(0001,1000 P (60)	-1 * 16012C180 (0001,1000) R (62)
625.087914 =	2 * 16014C160	(0001,1000 P (64)	-1 * 16013C160 (0001,0200) P (30)

CO₂ ISOTOPE LASER FREQUENCY SYNTHESIS

$$\nu_S \approx 625.0 \pm 0.1 \text{ cm}^{-1}$$

$$\nu_S \approx 18.750 \pm 0.003 \text{ THz}$$

$$\lambda_S \approx 16.00000 \pm 0.00256 \mu\text{m}$$

18-5-6029

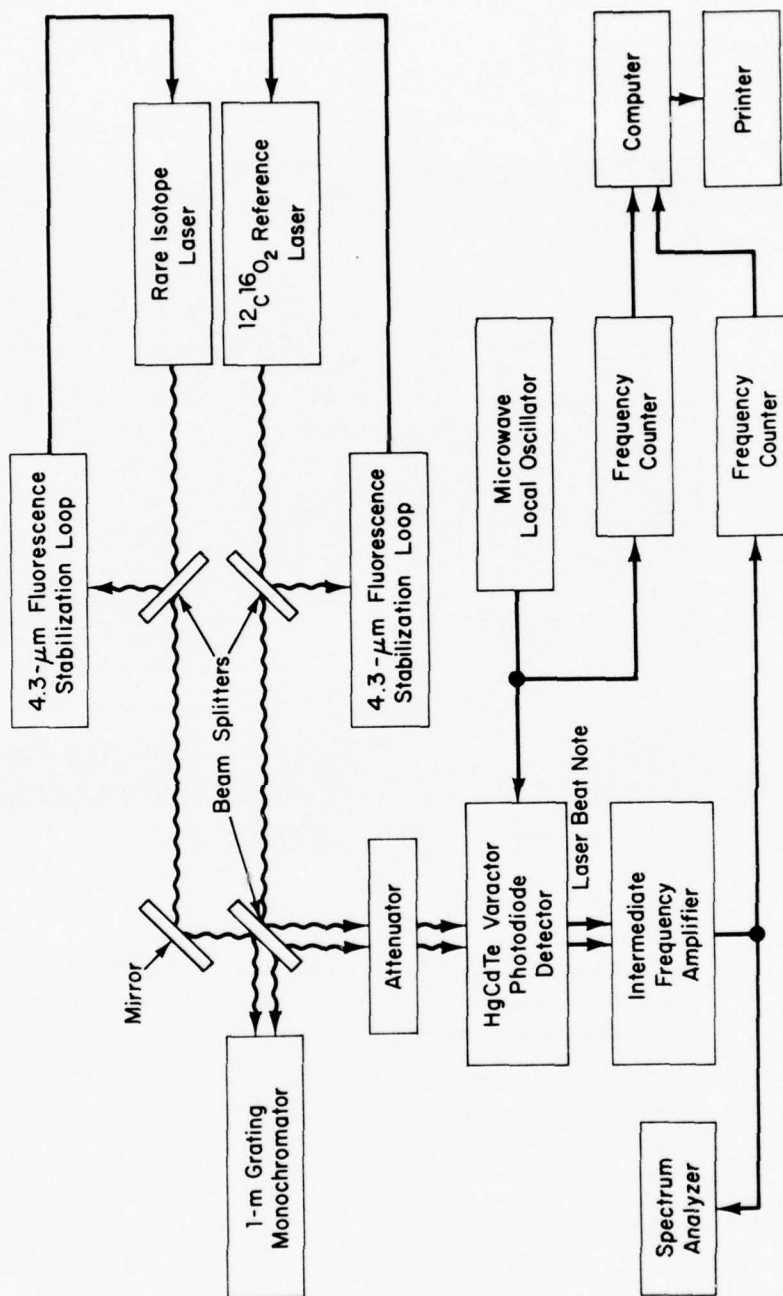
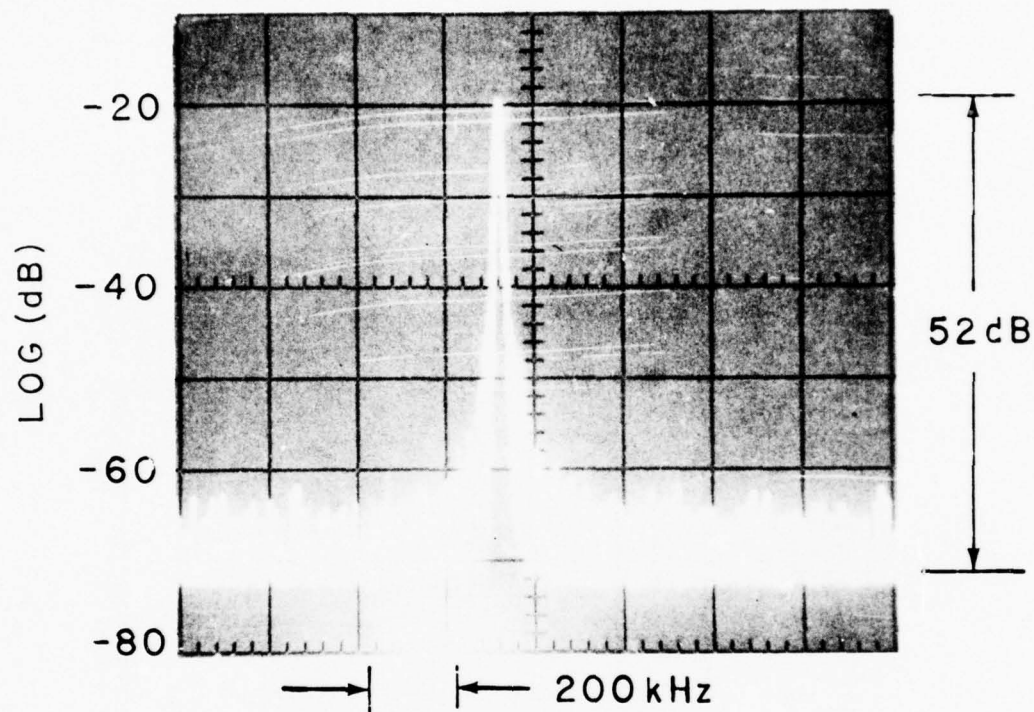


FIGURE 1

FIGURE 2



2. 24,410.301 MHz beat of $^{16}\text{C}^{12}\text{O}^{18}\text{O}$ Laser 001-I P(12) and $^{12}\text{C}^{16}\text{O}_2$ Laser 001-I P(6) Transitions

Power Levels into Photodiode:

$^{12}\text{C}^{16}\text{O}_2$ Laser: 0.42 mW

$^{16}\text{O}^{12}\text{C}^{18}\text{O}$ Laser: 0.48 mW

Second Harmonic of Microwave L. O. is Used

10kHz Noise Bandwidth

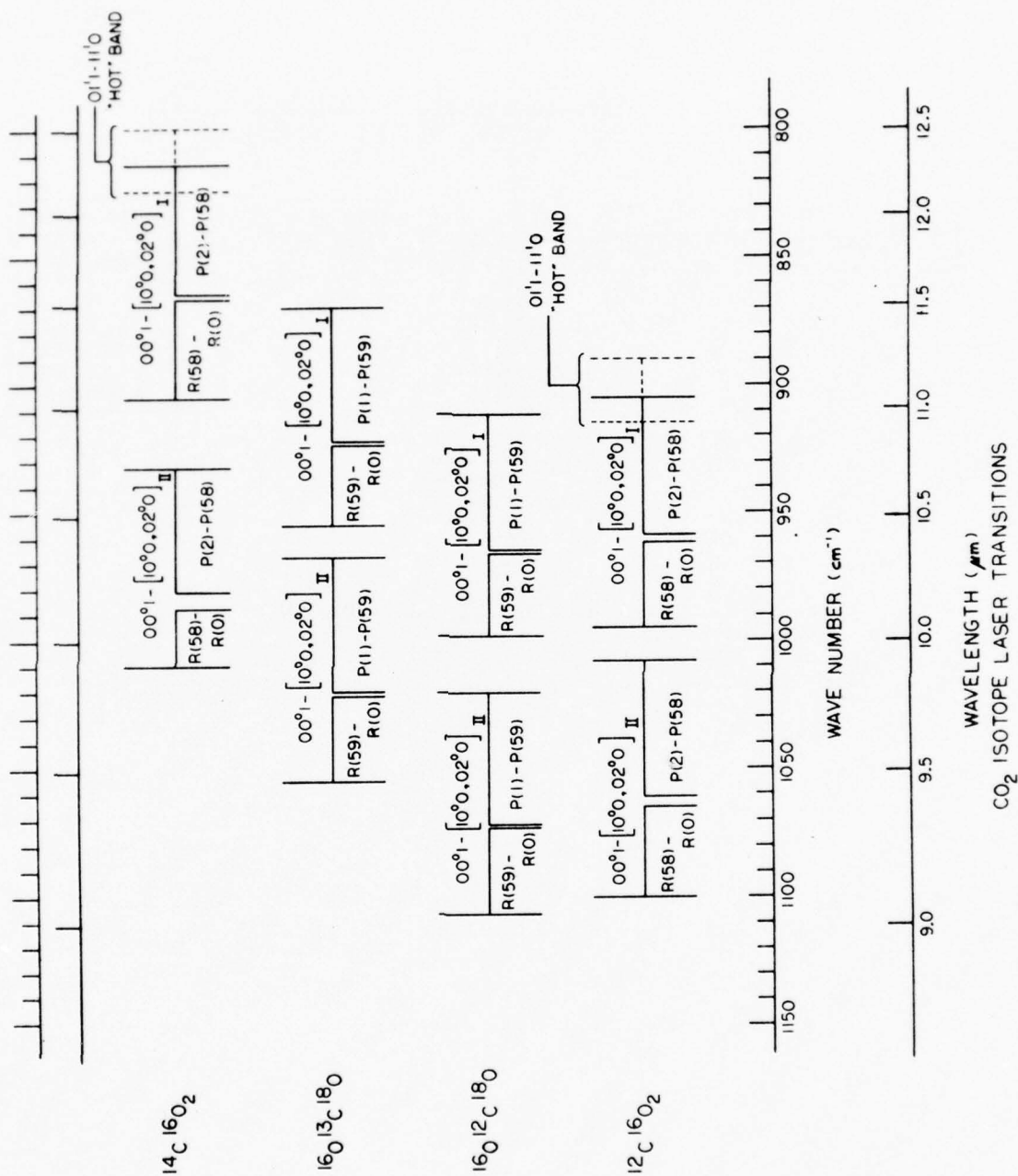
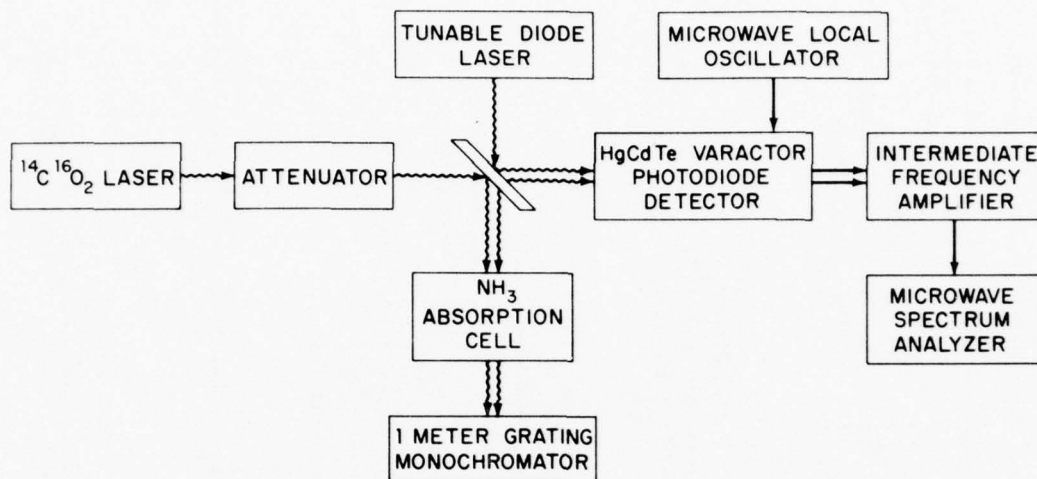


FIGURE 3

FIGURE 4

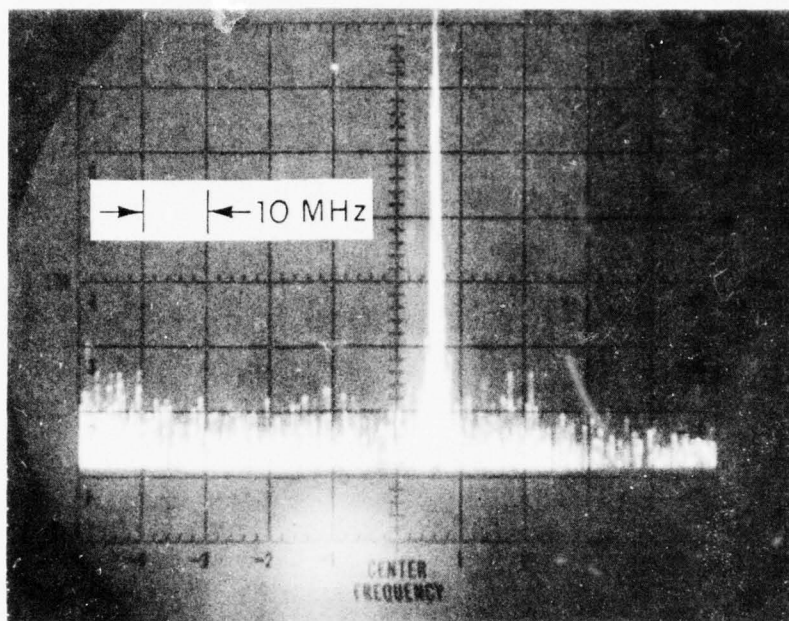
18-5-7111



12.1 μm WAVELENGTH CALIBRATION

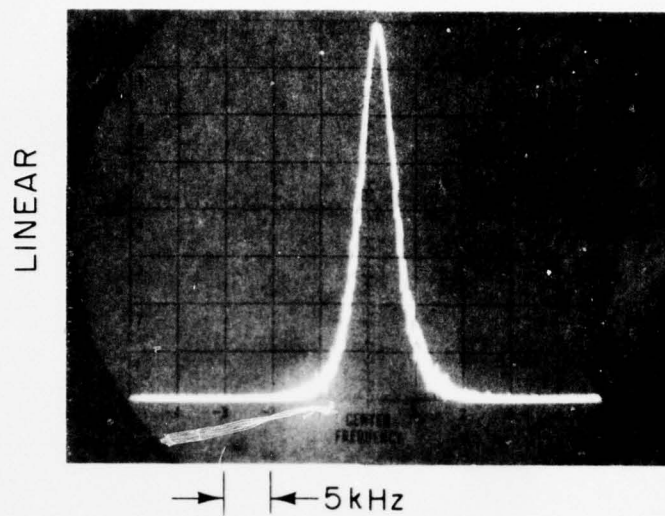
FIGURE 5

-5-7112



6,775 MHz beat note of a $^{14}\text{C}^{16}\text{O}_2$ laser $00^0_1 - [10^0_0, 02^0_0]_1$
band P – transition and a diode laser tuned to an ammonia
absorption line at $12.1\ \mu\text{m}$

FIGURE 6



3,165 MHz BEAT FREQUENCY OF A
 $^{12}\text{C}^{16}\text{O}_2$ 001-I BAND R(18) TRANSITION
WITH A $^{14}\text{C}^{16}\text{O}_2$ LASER LINE

I.F. BANDWIDTH : 3 kHz

Advances in CO₂ Laser Stabilization
Using the 4.3 μ m Fluorescence Technique^{*}

by

Charles Freed

and

Robert G. O'Donnell

M.I.T. Lincoln Laboratory
Lexington, Massachusetts

PREPRINT

To be published in the Proceedings of the 2nd Symposium on Frequency Standards and Metrology held 5 - 7 July 1976, Copper Mountain, CO.

* This work was sponsored by the Advanced Research Projects Agency of the Department of Defense and in part by U. S. Energy Research and Development Administration.

Advances in CO₂ Laser Stabilization
Using the 4.3 μ m Fluorescence Technique*

by

Charles Freed and Robert G. O'Donnell

M.I.T. Lincoln Laboratory
Lexington, Massachusetts

ABSTRACT

Significant improvement in signal-to-noise ratios is achieved with new, low pressure CO₂ stabilization cells external to the lasers. A time domain fractional frequency stability of $\sigma_y(\tau) \approx 6 \times 10^{-12} \tau^{-1/2}$ was measured with independently line-center locked 1.5 meter grating controlled CO₂ lasers. Accurate, repeatable determination of pressure shift is demonstrated.

*This work was sponsored by the Advanced Research Projects Agency of the Department of Defense and in part by U. S. Energy Research and Development Administration.

Advances in CO₂ Laser Stabilization Using the 4.3 μ m Fluorescence Technique*

by

Charles Freed and Robert G. O'Donnell

M.I.T. Lincoln Laboratory
Lexington, Massachusetts

INTRODUCTION

At the 1976 Boulder Conference on Precision Electromagnetic Measurements we described¹ the absolute frequency calibration of CO₂ isotope laser transitions with the two channel laser heterodyne system shown in Fig. 1. This paper will discuss the stabilization technique and the frequency stability achieved with the equipment indicated in Fig. 1.

It was previously shown^{2,3} that CO₂ lasers can be frequency stabilized by using the standing-wave saturation resonances in a low-pressure, room-temperature, pure CO₂ absorber via the intensity changes observed in the collisionally-coupled spontaneous emission band at 4.3 μ m. It was also demonstrated that the frequency shift due to changes in pressure is very small in CO₂, typically about 100 Hz/mTorr.

In the initial experiments, a short gas cell with a total absorption path of about 3 cm was placed inside the cavity of each stable CO₂ laser^{3,4} with a Brewster angle window separating the cell from the laser gain tube. Pure CO₂ gas at various pressures was introduced inside the sample cell. A sapphire window at the side of the sample cell allowed the observation of the 4.3 μ m spontaneous emission signal with a liquid-nitrogen-cooled InSb detector. The detector element was about 1.5 cm from the path of the laser beam in the sample cell. In order to reduce the broadband noise caused by background radiation, the detector placement was chosen to be at the center of curvature of a gold-coated spherical mirror which was internal to the gas absorption cell. Essentially identical experimental arrangements of CO₂ lasers, internal absorption cells, and InSb 4.3 μ m fluorescence detectors have been used in more recent experiments by Petersen et al,⁵ Meyer and Rhodes,⁶ and also by Woods and Joliffe⁷ who used similar but external absorption cells.

*This work was sponsored by the Advanced Research Projects Agency of the Department of Defense and in part by U. S. Energy Research and Development Administration.

SIGNAL-TO-NOISE RATIO AT 4.3 μm

In the CO_2 isotope calibration system shown by Fig. 1, we use improved CO_2 stabilization cells external to the lasers.

In the new design, the low pressure gas cell, the LN_2 -cooled radiation collector, and the IR detector are all integral parts of one evacuated housing assembly. This arrangement minimizes signal absorption by windows and eliminates all other sources of absorption. Because of the vacuum enclosure, diffusion of other gases into the low-pressure gas reference cell is almost completely eliminated; therefore, the time period available for continuous use of the reference gas cell is greatly increased and considerable less time has to be wasted on repumping and refilling procedures. One LN_2 fill will last at least 24 hours. Figure 2 schematically illustrates the new external reference gas cell used in the 4.3 μm fluorescence stabilization loop.

With the new cells significantly larger signal collection efficiency is achieved simultaneously with a great reduction of noise due to background radiation, which is the primary limit for high-quality InSb photovoltaic detectors. We have evaluated and tested several large area InSb detectors and determined that LN_2 -cooled background greatly diminished 1/f noise in addition to the expected reduction in white noise due to the lower temperature background radiation. In comparison with previously published results, we obtained more than two orders of magnitude improvement of the signal-to-noise ratio in measuring the 4.3 μm fluorescence.

Figure 3 shows a typical recorder tracing of the observed 4.3 μm intensity change as the laser frequency is tuned across the 10.59 μm P(20) line profile with 0.034 Torr pressure of CO_2 absorber gas. The standing wave saturation resonance appears in the form of a narrow resonant 16.4% "dip" in the 4.3 μm signal intensity. The broad background curve is due to the laser power variation as the frequency is swept within its oscillation bandwidth. Since collision broadening in the CO_2 absorber is about 7.6 MHz/Torr FWHM,^{2,6} in the limit of very low gas cell pressure the linewidth is determined primarily by power broadening and by the molecular transit time across the diameter of the incident beam. The potentially great improvements in signal-to-noise ratio, in power and transit time broadening and in short-term laser stability were the

motivating factors that lead to the choice of stabilizing cells external to the laser's optical cavity.

The one disadvantage inherent with the use of external stabilizing cells is that appropriate precautions must be taken to avoid optical feedback into the lasers to be stabilized.

For frequency reference and long term stabilization it is convenient to obtain the derivative of the 4.3 μm emission signal as a function of frequency. This 4.3 μm signal derivative may be readily obtained by a small dithering of the laser frequency as we slowly tune across the resonance in the vicinity of the absorption line center frequency. With the use of standard phase-sensitive detection techniques we can then obtain the 4.3 μm derivative signal to be used as a frequency discriminator. Figure 4 shows such a 4.3 μm derivative signal as a function of laser tuning near the center frequency of the 10.59 μm P(20) transition.

Figure 4 also illustrates the signal and noise level amplitudes we have chosen to define the signal-to-noise ratios of the frequency discriminants in this paper. More than half of the noise was caused by background photon current noise $i_p^2 = 2 e I_p \Delta f$, with the remainder primarily due to residual $1/f$ noise. As Fig. 4 shows, the noise levels were chosen near the peak-to-peak rather than the r.m.s. value. A single RC filter with a 0.1 sec risetime was used to measure all the 4.3 μm signal and noise results shown in this paper. Thus, the S/N data presented here were obtained with a noise bandwidth which was twenty times wider than the one we have used in our previously published experiments.^{2,4} Obviously, we could have shown much larger S/N values by using longer noise averaging times; nevertheless the wide bandwidth data are considered more appropriate for usability in closed loop stabilization schemes.

Figure 5 shows another 4.3 μm derivative signal with a ± 20 kHz frequency dither which we used to lock one laser to the center of the P(20) absorption profile. Figure 6 shows the spectrum analyzer display of the beat note of two lasers. One of the lasers was line-center locked by using the discriminant shown in Fig. 5, while the other laser was free running with a frequency offset of about 8 MHz. If both lasers are synchronously modulated at a 260 Hz rate with a ± 20 kHz peak deviation of the 10.59 μm P(20) signal, the beat note appears as a relatively narrow single spectral line shown in the left half of

Fig. 6. The right half of Fig. 6 illustrates a typical FM signal spectrum which results when the modulation signal is disconnected from the free running laser. The lasers remained locked to the line center with as little as ± 2 kHz frequency dither. Respective rise times of 0.001 and 0.03 to 1.5 seconds were used in the phase sensitive detector and in the high voltage integrating amplifier of the servo loop.⁸

Figure 7 illustrates the signal, noise and S/N obtained with ± 100 kHz dithering of the laser. Figure 8 provides a summary of the signal-to-noise ratios as a function of peak frequency deviation at a 260 Hz rate. The results summarized in Fig. 8 were obtained with a $^{12}\text{C}^{16}\text{O}_2$ 10.59 μm P(20) laser power of about 1.75 watts. The absorption cell diameter, the beam diameter (at the 1/e field) and beam divergence were about 22.2 mm, 11.8 mm and 1.5×10^{-3} radians, respectively. The CO_2 cell pressure was purposefully chosen to be about 0.034 Torr to provide easy comparison with previously published results.^{2,4,5,6}

The relatively slow decay^{9,10} of the spontaneous 4.3 μm radiation arising from the $(00^0_1) \rightarrow (00^0_0)$ transition seriously limits the maximum frequency that can be effectively used to modulate the CO_2 lasers. Figure 9 clearly illustrates the loss of the 4.3 μm signal with increasing modulation frequency. The 4.3 μm decay rate is primarily determined by cell pressure and geometry. Consideration of detector 1/f noise may well dictate an optimum modulating frequency which is higher than would be indicated by considering the signal alone. As an example, Fig. 10 shows the signal, noise and S/N as a function of modulation frequency for one of our reference cells. From Fig. 10 it is clear that at 0.034 Torr pressure the optimum modulating frequency is approximately 500 Hz, in spite of some loss of signal at this frequency.

FREQUENCY STABILITY AND REPRODUCIBILITY

In order to investigate in the most direct fashion the various parameters affecting frequency stability, we carried out extensive measurements of the Allan Variance on the 2,697.86 MHz beat frequency between the $^{12}\text{C}^{16}\text{O}_2$ $00^0_1 - [10^0_0, 02^0_0]_I$ band P(20) and the $^{13}\text{C}^{18}\text{O}_2$ $00^0_1 - [10^0_0, 02^0_0]_I$ band R(24) laser transitions.¹¹ By using two different CO_2 isotope lines, frequency pulling due to optical feedback was avoided and the 2,697 MHz beat frequency output of the HgCdTe photodiode was directly measured by a microwave frequency counter; thus only two independently lockable lasers and a single microwave frequency counter were

utilized in the experiments to be described in this section (Note that Fig. 1 indicates a separate microwave local oscillator and a second counter; neither of these were necessary for the stability measurements.)

Since each laser was assumed to contribute equally to the instability, the measured Allan Variance was divided by $\sqrt{2}$ times the laser frequency (2.8306×10^{13} Hz) in order to derive the fractional frequency stability for a single laser as a function of sample time, τ (gating time of the frequency counter).

In compliance with the "Truth in Packaging" dictates¹² that the sample size, m , be stated with the results, Table I gives the sample size, m , for each observation time, τ , used to obtain the Allan Variance.

τ (seconds)	0.1	0.2	0.4	0.7	1.0	2	5	10	25	50	100	250	500	1000
m	101	101	101	101	101	51	26	26	11	3	3	3	3	2

Table I. Sample Size, m , as a Function of Sample Time, τ .

The stability of the lasers may be best summarized by Fig. 11 where each circle or cross represents an Allan Variance measurement based on a sample size, m , as specified in Table I above.

The fractional stability of the beat note of the two lasers under free running conditions is denoted by crosses and may be reasonably well approximated by σ_y (unlocked) $\approx 10^{-10} \times \tau^{0.72}$ which of course indicates the drift rate of the lasers relative to each other.

The circles represent the results obtained with each laser independently locked to its own reference absorption cell filled with 40 mTorr of $^{12}\text{C}^{16}\text{O}_2$ and $^{13}\text{C}^{18}\text{O}_2$, respectively.

As Fig. 11 indicates, there were three consecutive sets of measurements made, each based on m samples for any given observation time, τ . The locked laser stability may be described by σ_y (locked) $\approx 6 \times 10^{-12} \tau^{-1/2}$.

Thus, the instability of the lasers became less than 1×10^{-12} for sample times $\tau \geq 40$ seconds. A fractional stability of 10^{-12} corresponds to $\sigma_y \approx 28$ Hz fluctuation in the laser frequency. Since the piezoelectric mirror tuning rate is about 200 kHz/volt, the phase sensitive detector output stability (drift) must be less than 150 μ V to achieve 1×10^{-12} long-term stability. Such low, long-term drift was clearly beyond the capability of the ten year old lock-in amplifiers used to obtain these results; therefore, the measurement of longer term stability with larger sample sizes was not seriously pursued in the current phase of our experiments. However, the stability we did obtain was quite sufficient to carry out accurate and reproducible measurement of pressure shift in CO_2 .

In the pressure shift experiments both lasers are locked to their individual reference cells, and the shift in the beat frequency is measured as a function of pressure change in one of the cells, with the pressure held constant in the second cell in order to obtain a stable reference laser frequency.

Figure 12 shows the last two digits of the $2,697,862 \pm 6$ kHz beat frequency of the $^{12}\text{C}^{16}\text{O}_2$ laser $00^0_1 - [10^0_0, 02^0_0]_I$ - band P(20) and the $^{13}\text{C}^{18}\text{O}_2$ laser $00^0_1 - [10^0_0, 02^0_0]_I$ - band R(24) transitions as a function of pressure in the $^{12}\text{C}^{16}\text{O}_2$ reference cell. Each circle in Fig. 12 is based on an observation time of $\tau = 10$ seconds and a sample size of $m = 26$. As Fig. 12 indicates, two independent, consecutive sets of measurements give results which are barely distinguishable from each other and are within one $\sigma_y(\tau)$ of the solid line. A straight line fitting (by the least-squares method) of the data between 0 and 60 mTorr yields a -108.6 Hz/mTorr frequency change with increasing pressure in the $^{12}\text{C}^{16}\text{O}_2$ reference cell (red shift). The pressure shift becomes larger and nonlinear at higher pressures, but for the purpose of frequency stabilization only the low pressure region is of interest. It is rather interesting to note that our original 1970 estimate^{2,3} was also about 100 Hz/mTorr red shift for the same P(20) laser transition.

Analogous data for the $^{13}\text{C}^{18}\text{O}_2$ $00^0_1 - [10^0_0, 02^0_0]_I$ - band R(24) transition gave a 168.6 Hz/mTorr red shift in the 0 - 60 mTorr pressure range. Neither repeated breaking and resetting of the frequency lock, nor refilling of the lasers and the reference cells altered the results shown in Figs. 11 and 12.

CONCLUSIONS

The data presented in this paper clearly show significant advances in CO₂ laser stabilization using the 4.3 μ m fluorescence technique. The time-domain frequency stability data of Fig. 11 are quite consistent with the spectral density measurements presented at the Seminar on Frequency Standards and Metrology in Quebec (See Fig. 5).⁴ It is noteworthy that the frequency stability shown in this paper was achieved with relatively large, 1.5 meter, grating controlled, LR-35 invar lasers (See Fig. 3 in Reference 4) with ± 100 kHz synchronous frequency modulation of the outputs. We have previously demonstrated far better spectral purity with smaller, super-invar^{13,14} cavity lasers (See Figs. 1 and 4 in Reference 4.) In the next phase of our experiments the use of super-invar lasers in conjunction with larger diameter stabilizing cells and ultra-stable electronics will undoubtedly result in at least one order of magnitude improvement over the time domain stability shown in Fig. 11.

ACKNOWLEDGMENTS

The authors are deeply appreciative to A. H. M. Ross for many helpful discussions, and to D. L. Spears for providing the fast HgCdTe varactor-photodiodes.

REFERENCES

1. C. Freed, R. G. O'Donnell, and A. H. M. Ross, "Absolute Frequency Calibration of the CO_2 Isotope Laser Transitions" to be published in the Dec. 1976 issue of IEEE Trans. Instrum. Meas.
2. C. Freed and A. Javan, "Standing-Wave Saturation Resonances in the $10.6 \mu\text{m}$ Transitions Observed in a Low-Pressure Room-Temperature Absorber Gas," Appl. Phys. Lett. 17, pp 53-56, 15 July 1970.
3. C. Freed and A. Javan, "Standing-Wave Saturation Resonances in Room Temperature CO_2 $10.6 \mu\text{m}$ Absorption Lines," Paper 4.4 presented at the 1970 Sixth International Quant. Elect. Conference, September 1970, Kyoto, Japan.
4. C. Freed, "Designs and Experiments Relating to Stable Lasers," Proceedings of the Frequency Standards and Metrology Seminar, University Laval, Quebec, Canada, pp. 226-261, September 1, 1971.
5. F. R. Petersen, D. G. McDonald, J. D. Cupp, and B. L. Danielson, "Accurate Rotational Constants, Frequencies, and Wavelengths from $^{12}\text{C}^{16}\text{O}_2$ Lasers Stabilized by Saturated Absorption," Proc. of the Laser Spectroscopy Conference, June 25-29, 1973, Vail, Colorado.
6. T. W. Meyer, "Line Broadening and Collisional Studies of CO_2 Using the Techniques of Saturation Spectroscopy," Ph. D. Thesis, U. of California, Lawrence Livermore Laboratory, UCRL-51561, April 1974.
7. P. T. Woods and B. W. Joliffe, "Stable Single-Frequency Carbon Dioxide Lasers," J. of Physics E: Scientific Instruments 9, pp 395-402, 1976.
8. The author gratefully appreciates the correspondence and circuit diagrams which John Hall (of JILA, U of Colorado) provided. However, because of significant differences in detectors, piezoelectrics and modulation frequencies, we designed and constructed new circuitry specially tailored to the components we use.
9. M. Kovacs, D. Ramachandra Rao and A. Javan, "Study of Diffusion and Wall De-Excitation Probability of 00^0_1 State in CO_2), J. Chem. Phys. 48, No. 7, 3339-3341, April 1, 1968.
10. L. Doyennette, M. Margottin-Maclou, H. Gueguen, A. Carion and L. Henry, "Temperature Dependence of the Diffusion and Accomodation Coefficients in Nitrous Oxide and Carbon Dioxide Excited into the (00^0_1) Vibrational Level," J. Chem. Phys. 60, No. 2, 697-702, Jan. 15, 1974.

11. C. Freed, A. H. M. Ross and R. G. O'Donnell, "Determination of laser Line Frequencies and Vibrational-Rotational Constants of the $^{12}\text{C}^{18}\text{O}_2$, $^{13}\text{C}^{16}\text{O}_2$, and $^{13}\text{C}^{18}\text{O}_2$ Isotopes from Measurements of CW Beat Frequencies with Fast HgCdTe Photodiodes and Microwave Frequency Counters," J. Molecular Spectrosc. 49, 439 (1974).
12. J. A. Barnes, A. R. Chi, L. S. Cutler, D. J. Healey, D. B. Leeson, T. E. McGunigal, J. A. Mullen, Jr., W. L. Smith, R. L. Sydnor, R. F. C. Vessot, and G. M. R. Winkler, "Characterization of frequency stability," IEEE Trans. Instrum. Meas., IM-20, pp. 105-120, May 1971.
13. C. Freed, "Design and Short-Term Stability of Single-Frequency CO_2 Lasers," IEEE J. Quan. Elect. QE-4, pp. 404-408, June 1968.
14. J. W. Berthold III, S. F. Jacobs, and M. A. Norton, "Dimensional Stability of Fused Silica, Invar, and Several Ultralow Thermal Expansion Materials," Applied Optics Lett. 15, pp. 1898-9 August 1976. (A more detailed version of this paper will be published in the January 1977 issue of Metrologia.)

18-S-6029

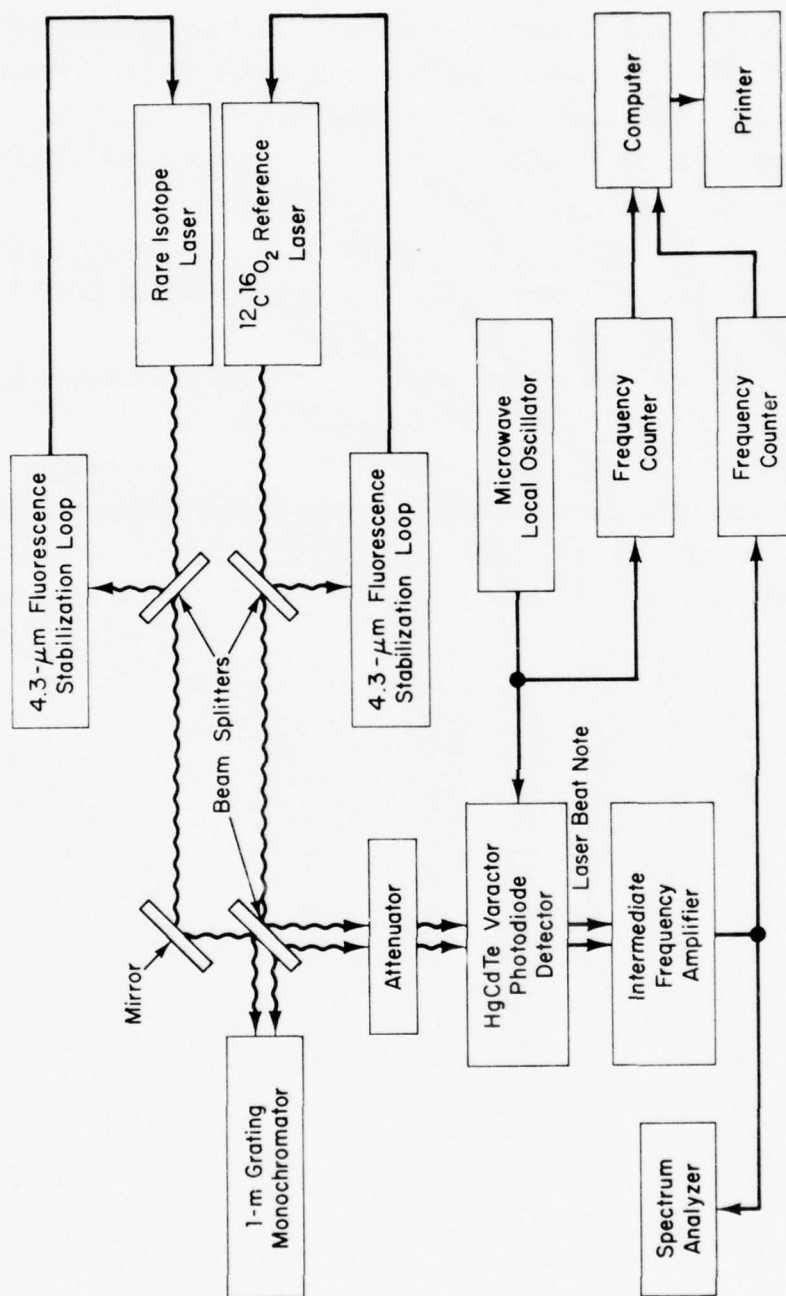


Fig.1. Two-channel Heterodyne System used to Determine CO_2 Isotope Laser Frequencies.

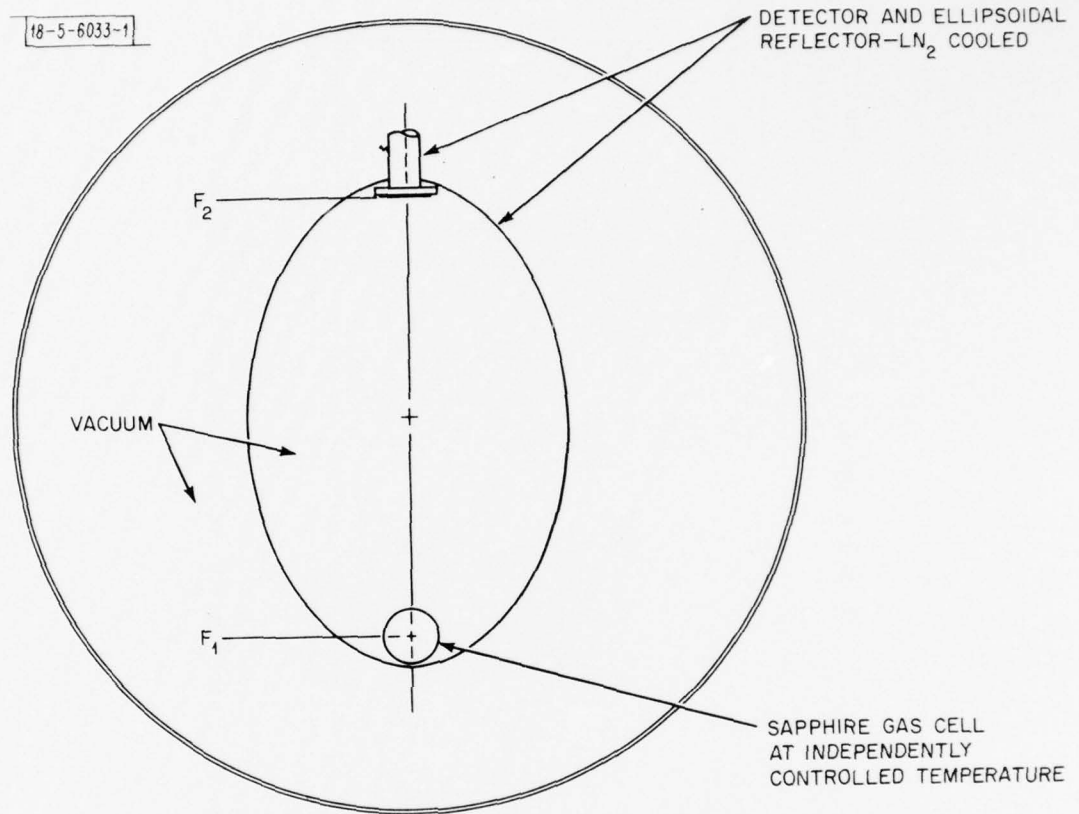


Fig.2. Schematic Illustration of the New External CO₂ Reference Gas Cell.

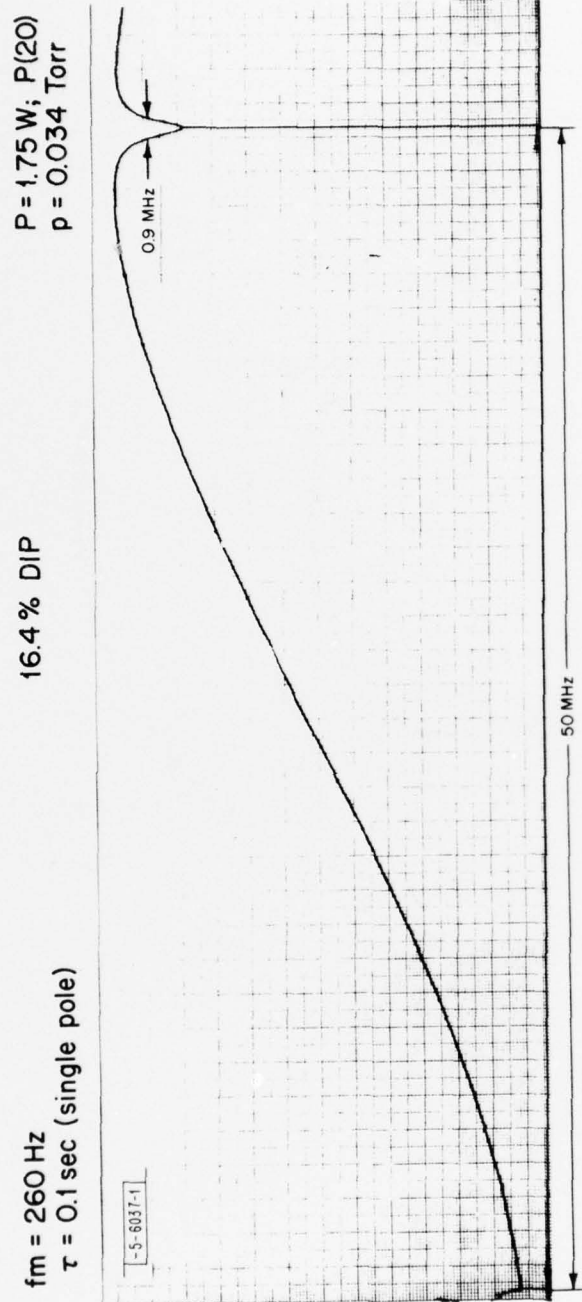


Fig.3. Recorder Tracing of the $4.3 \mu\text{m}$ Intensity Change Signal as A Function of Laser Frequency Tuning in the $P(20)$ Transition at $10.59 \mu\text{m}$.

S/N = 29

$\Delta f = \pm 5 \text{ kHz}$

$f_m = 260 \text{ Hz}$

$\tau = 0.1 \text{ sec (single pole)}$

$P_0 = 1.75 \text{ W, P(20); } 10.6 \mu\text{m}$

$p = 0.034 \text{ Torr}$

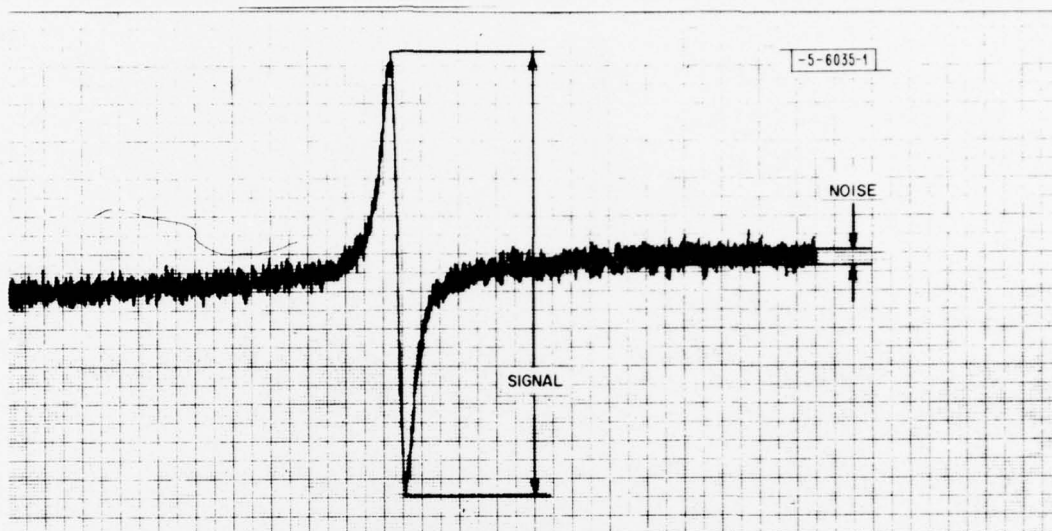


Fig.4. Recorder Tracing of the $4.3 \mu\text{m}$ Derivative Signal as a Function of Laser Frequency Tuning near the Center Frequency of the P(20) Transition at $10.59 \mu\text{m}$; the Frequency Dither is set to $\pm 5 \text{ kHz}$ at a 260 Hz Rate.

S/N = 97

$\Delta f = \pm 20$ kHz

$f_m = 260$ Hz

$\tau = 0.1$ sec (single pole)

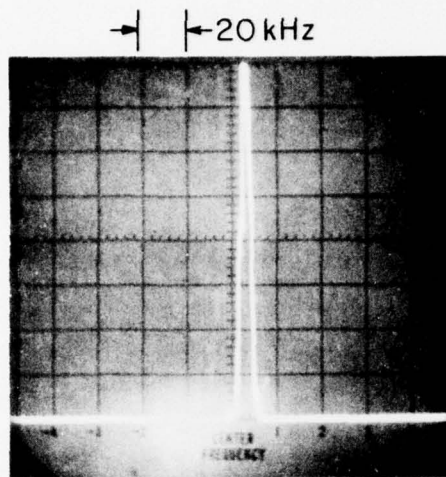
$P_0 = 1.75$ W; P(20); $10.6 \mu\text{m}$

$p = 0.034$ Torr

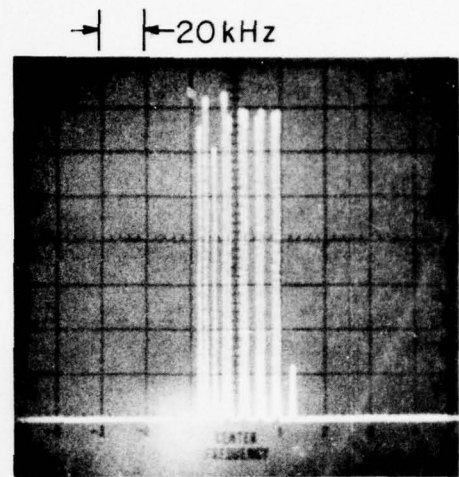


Fig.5. Recorder Tracing of the $4.3 \mu\text{m}$ Derivative Signal as a Function of Laser Frequency Tuning near the Center Frequency of the P(20) Transition at $10.59 \mu\text{m}$; the Frequency Dither is set to ± 20 kHz at a 260 Hz Rate.

-5-6028-1



Both Lasers Modulated
at 260 Hz



One Laser Modulated
at 260 Hz

Fig.6. Spectrum Analyzer Display of the Beat Note of Two Lasers with one Laser Locked to the Line Center and the Other Offset by 8 MHz and Free Running.

S/N = 480

$\Delta f = \pm 100 \text{ kHz}$

$f_m = 260 \text{ Hz}$

$\tau = 0.1 \text{ sec (single pole)}$

$P_0 = 1.75 \text{ W; P(20); } 10.6 \mu\text{m}$

$p = 0.034 \text{ Torr}$

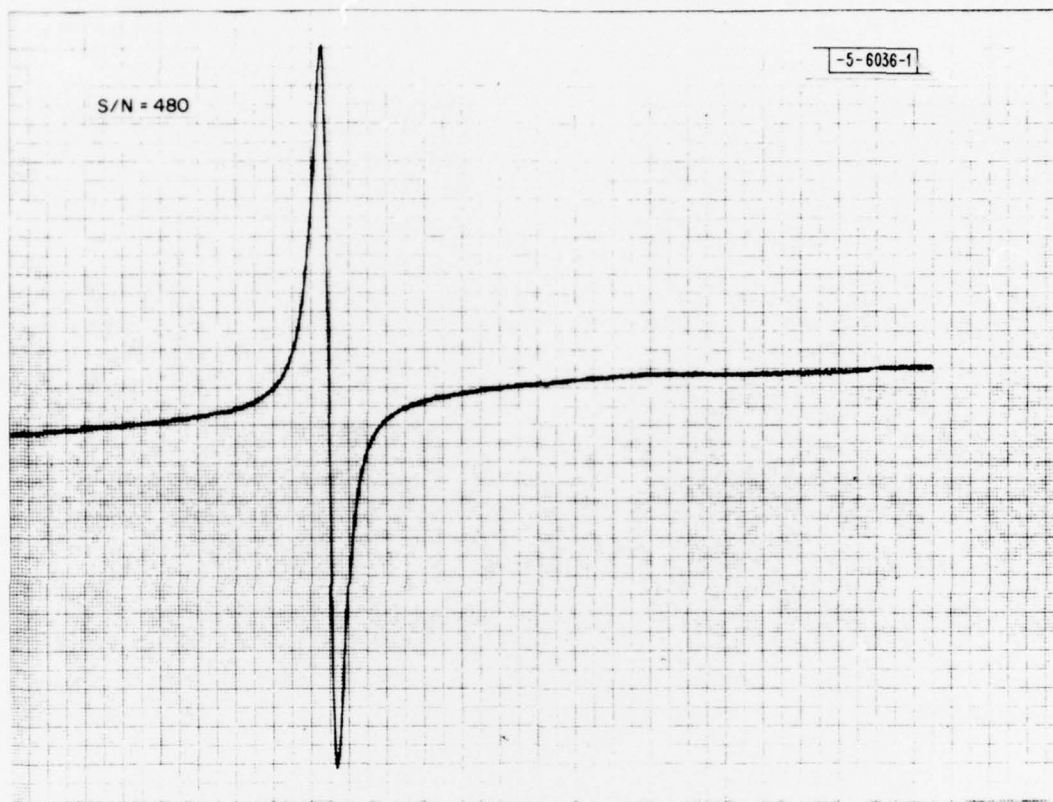


Fig.7. Recorder Tracing of the $4.3 \mu\text{m}$ Derivative Signal as a Function of Laser Frequency Tuning near the Center Frequency of the P(20) Transition at $10.59 \mu\text{m}$; the Frequency Dither is set to $\pm 100 \text{ kHz}$ at a 260 Hz Rate.

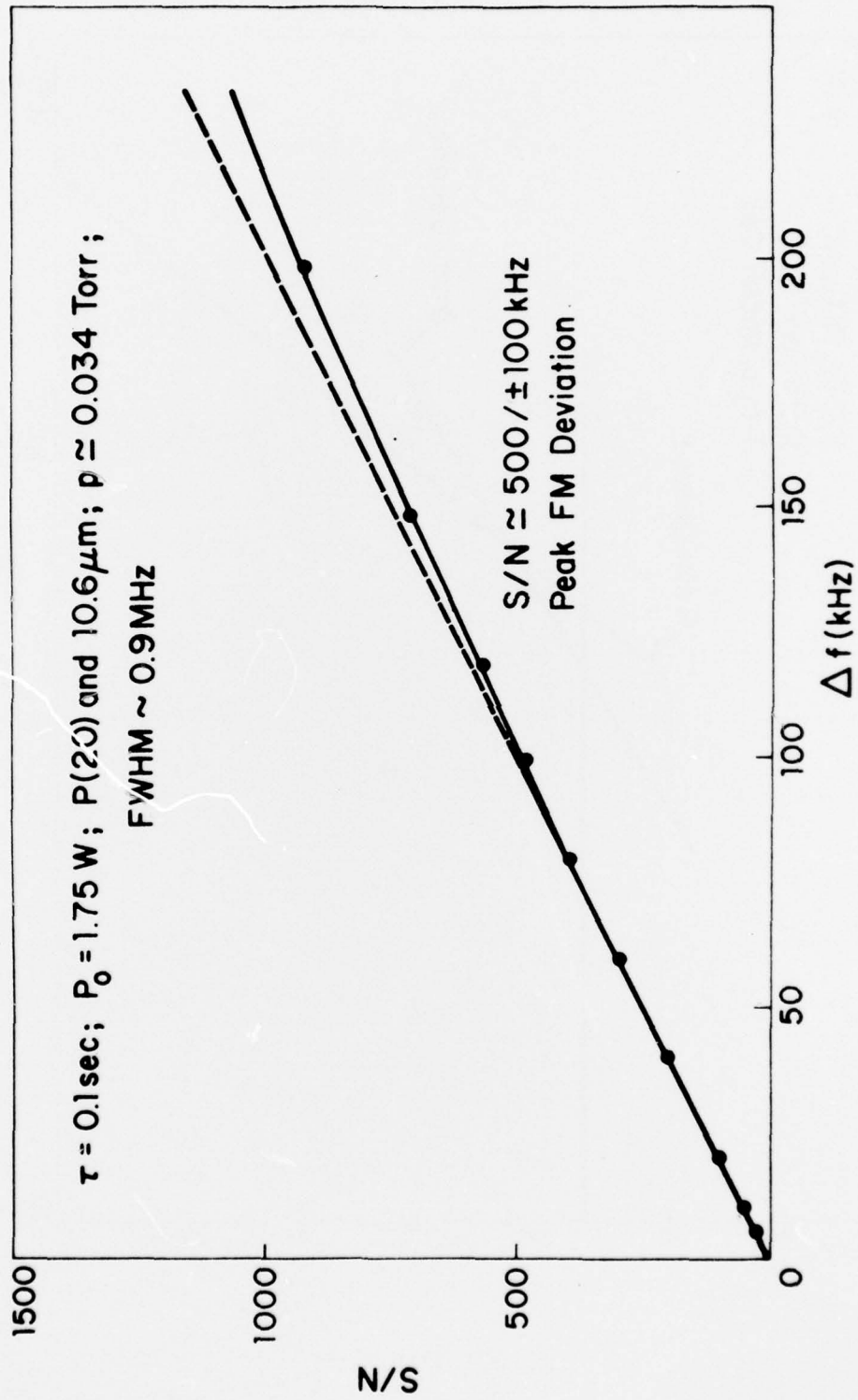


Fig.8. Signal-to-Noise Ratio as a Function of Peak Frequency Dither at a 260 Hz Rate.

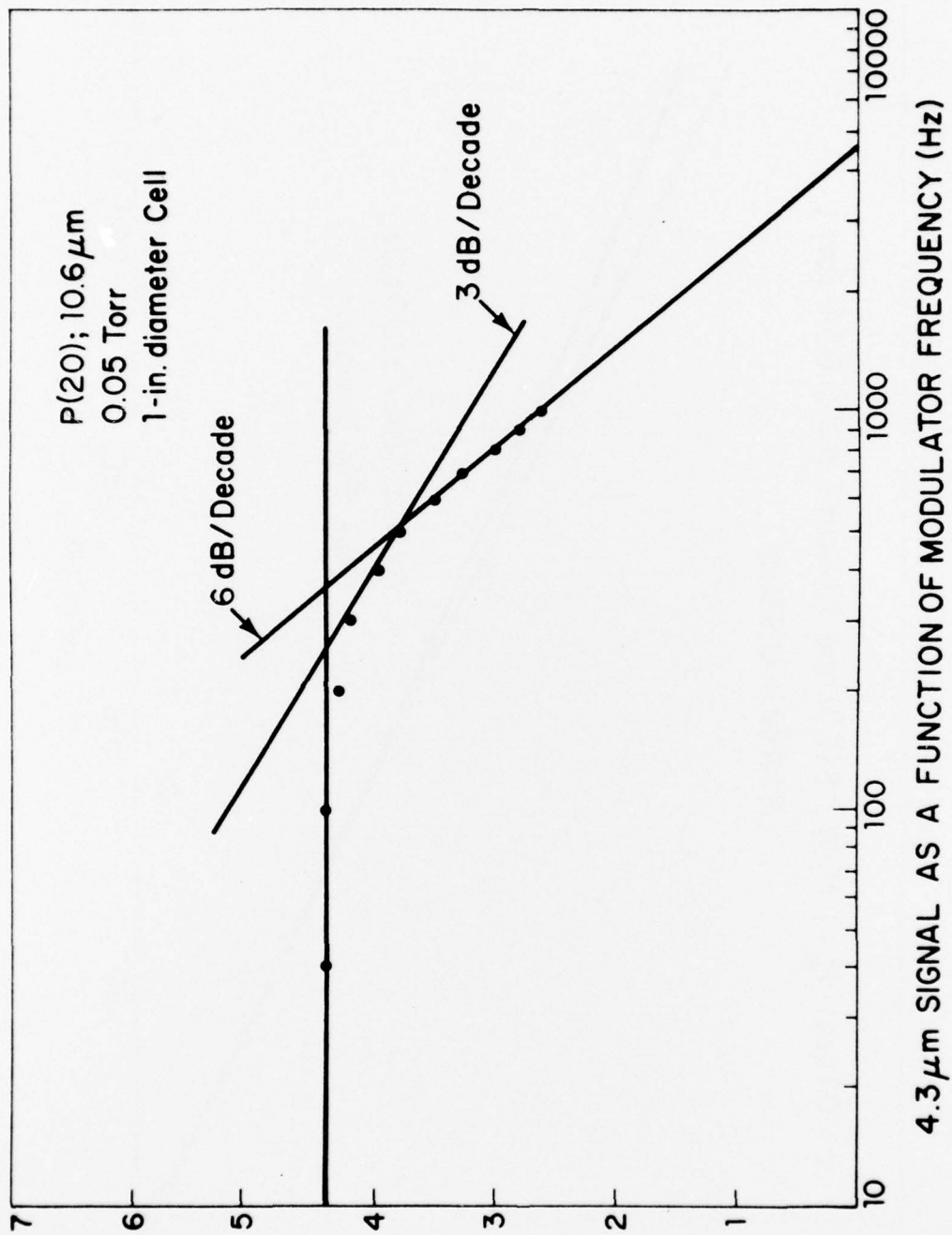


Fig.9. 4.3 μm Signal as Function of Modulator Frequency (Hz).

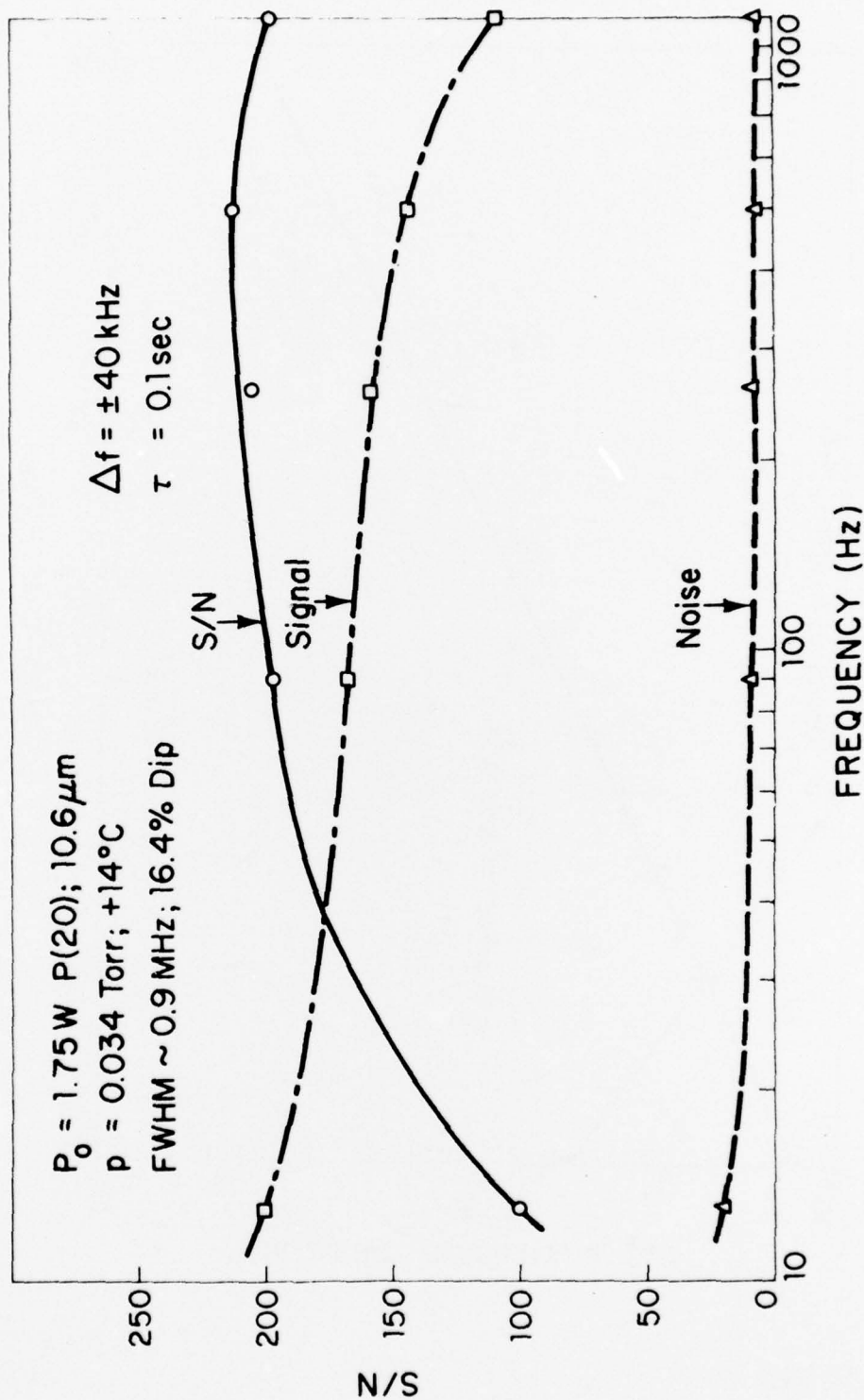


Fig.10. Signal, Noise and Signal-to-Noise Ratio as a Function of Modulation Frequency for a 22.2 mm Diameter Cell Filled with 0.034 Torr CO_2 .

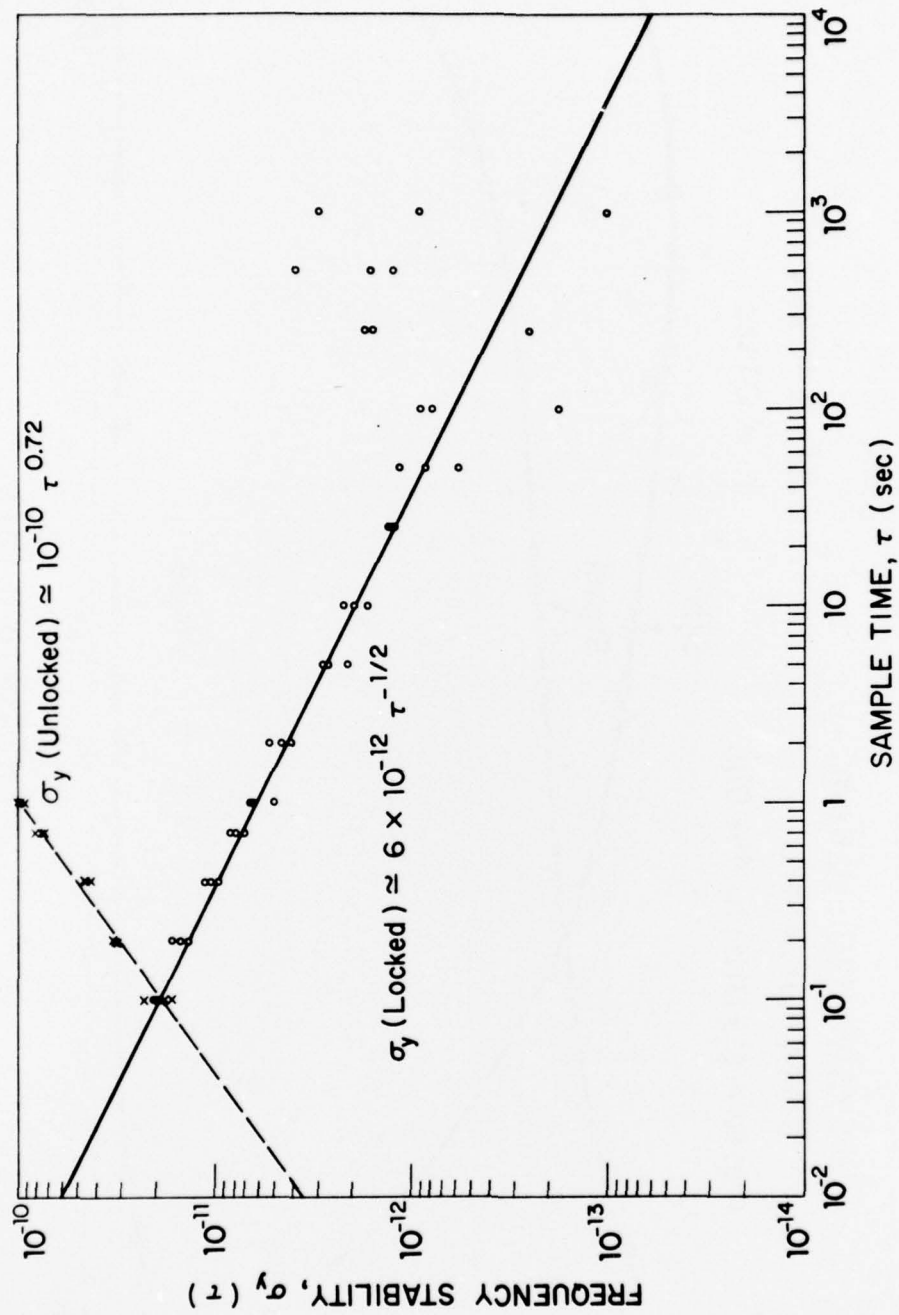


Fig.11. Time Domain stability of grating controlled CO₂ lasers.

18-5-7364

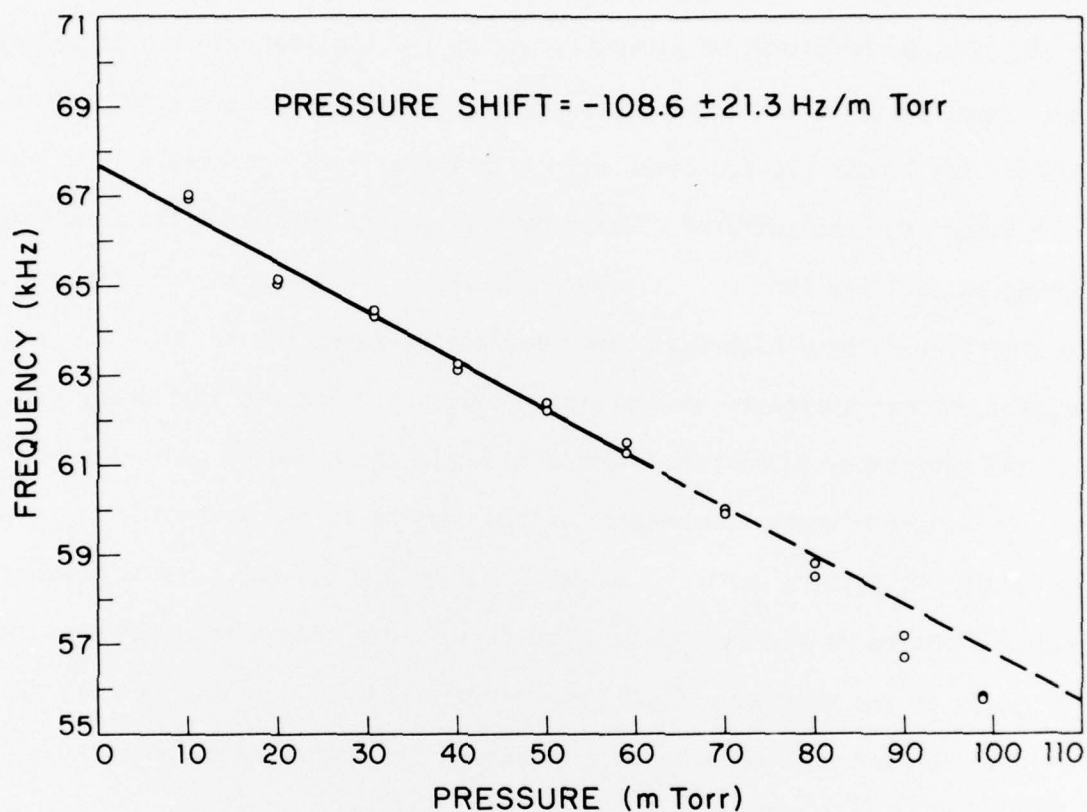


Fig.12. Variation of the 2,697,862 + kHz beat frequency as a function of pressure change in the $^{12}\text{C}^{16}\text{O}_2$ reference cell for the $00^0_1 - [10^0_0, 02^0_0]_I$ band P(20) transition.

4. MICROWAVE FREQUENCY SHIFTING

By scaling arguments it appears possible to demonstrate the shifting of $10.6 \mu\text{m}$ laser output by $\approx 0.5 \text{ cm}^{-1}$ with single sideband efficiency $> 1\%$. The cw technique we presently use is the application of a traveling microwave field in a waveguide structure containing single-crystal GaAs or CdTe. The linear electro-optic effect in the crystals generates two sidebands separated from the infrared carrier by the applied microwave frequency. By using essentially the same microwave structure and replacing the cw microwave source (100 W) by a high peak power magnetron (rated 100 kW, $0.5 - 3 \mu\text{s}$ pulse width) one can increase the conversion efficiency and use the linear dependence of the efficiency on microwave power to scale the expected conversion efficiencies.

Figure 4-1 shows a schematic of the crystal in the waveguide structure of width w , crystal width a , length L and height h . The crystal touches the top and bottom of the waveguide. The ratio w/a is chosen to match the phase velocity of the microwave field and the infrared field. With our crystal orientation the shifted frequency (sideband) is orthogonally polarized to the unshifted (carrier) frequency.

The linear electro-optic effect should have a single sideband conversion efficiency $E = \alpha P_M$ where P_M is the microwave power. For a GaAs crystal ($a = 5.6 \text{ mm}$, $h = 2.5 \text{ mm}$; $L = 6 \text{ cm}$) based on our cw measurements $\alpha \approx 2 \times 10^{-3} (\text{kW})^{-1}$. For a CdTe crystal ($a = 4.6 \text{ mm}$, $h = 2.5 \text{ mm}$, $L = 5 \text{ cm}$) $\alpha \approx 8 \times 10^{-3} (\text{kW})^{-1}$. This includes microwave and optical losses. Therefore a 10 kW microwave pulse should give $\approx 2\%$ conversion efficiency for GaAs, and 8% for CdTe.

Our initial tests have concentrated on the microwave breakdown problems which we feel will ultimately limit the conversion efficiency. We have used available polycrystalline CdTe (of the previously stated dimensions) in a

waveguide structure planned for the conversion tests. We found no breakdown at 10 kW, occasional breakdown at 15 kW, and frequent breakdown at 20 kW (all at 15.6 GHz). The CdTe was not damaged making it difficult to detect where the breakdowns occur. Due to the success at 10 kW we plan to measure optical conversion efficiencies using an AR-coated single-crystal piece of GaAs on hand. Figure 4-2 shows a schematic of the experimental layout. The polarizer following the modulator (frequency shifter) uses four plates of Ge at Brewster's angle to reflect the carrier into an absorber while transmitting the sideband. The Fabry-Perot is used as a narrowband infrared filter to select (and identify) one sideband. The detector is Cu:Ge with a ≈ 20 MHz response to detect the 1 μ s pulse.

An obvious limitation that can occur is damage to the AR coating on the crystal in the presence of the microwave field due to its electrical conductivity.

We plan to purchase a single crystal of CdTe to improve the efficiency and explore techniques to improve single-sideband efficiency once initial results are obtained.

G. M. Carter
C. Freed

Figure Captions:

- 4-1 Schematic representation of the crystal waveguide structure. E_o , E_s , E_m are the carrier, sideband, and microwave fields, respectively. \vec{k}_o , \vec{k}_m are the propagation vectors for the carrier and microwave fields. Dimensions not to scale.
- 4-2 Schematic of experimental arrangement for sideband generation and measurement.

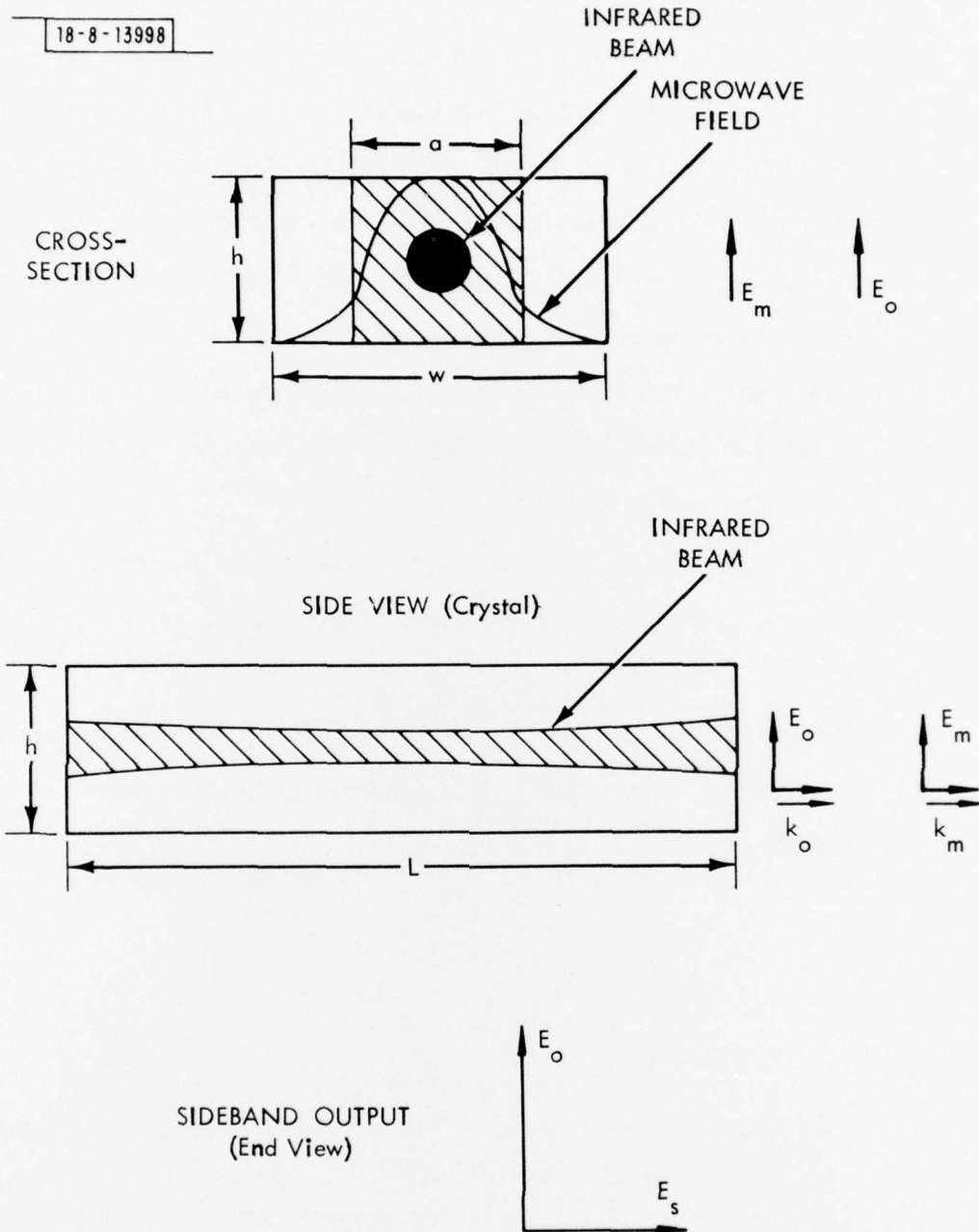


Fig.4-1

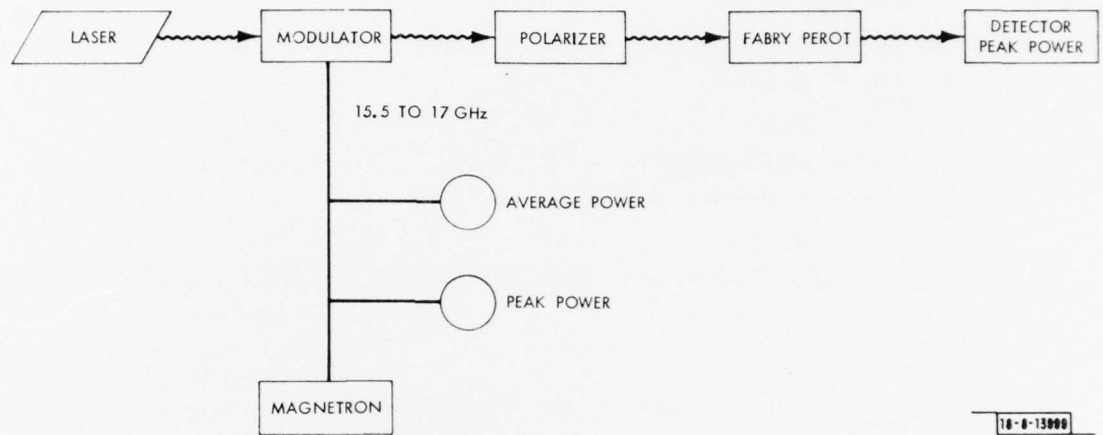


Fig.4-2

UNCLASSIFIED

SECURITY CLASSIFICATION OF THIS PAGE (When Data Entered)

REPORT DOCUMENTATION PAGE		READ INSTRUCTIONS BEFORE COMPLETING FORM
1. REPORT NUMBER ESD-TR-76-347	2. GOVT ACCESSION NO.	3. RECIPIENT'S CATALOG NUMBER
4. TITLE (and Subtitle) Laser Development in Support of the JUMPer Program for Laser Isotope Separation		5. TYPE OF REPORT & PERIOD COVERED Semiannual Report 1 July - 31 December 1976
		6. PERFORMING ORG. REPORT NUMBER
7. AUTHOR(s) Alan L. McWhorter		8. CONTRACT OR GRANT NUMBER(s) F19628-76-C-0002
9. PERFORMING ORGANIZATION NAME AND ADDRESS Lincoln Laboratory, M.I.T. P.O. Box 73 Lexington, MA 02173		10. PROGRAM ELEMENT, PROJECT, TASK AREA & WORK UNIT NUMBERS Project No. 920D
11. CONTROLLING OFFICE NAME AND ADDRESS Air Force Systems Command, USAF Andrews AFB Washington, DC 20331		12. REPORT DATE 31 December 1976
		13. NUMBER OF PAGES 70
14. MONITORING AGENCY NAME & ADDRESS (if different from Controlling Office) Electronic Systems Division Hanscom AFB Bedford, MA 01731		15. SECURITY CLASS. (of this report) Unclassified
		15a. DECLASSIFICATION DOWNGRADING SCHEDULE
16. DISTRIBUTION STATEMENT (of this Report) Approved for public release; distribution unlimited.		
17. DISTRIBUTION STATEMENT (of the abstract entered in Block 20, if different from Report)		
18. SUPPLEMENTARY NOTES None		
19. KEY WORDS (Continue on reverse side if necessary and identify by block number) JUMPer Program infrared nonlinear crystals CO ₂ lasers laser isotope separation optically pumped lasers		
20. ABSTRACT (Continue on reverse side if necessary and identify by block number) This report covers in detail the research and development work carried out by M.I.T. Lincoln Laboratory for the U.S. Energy Research and Development Administration in support of the JUMPer program at the Los Alamos Scientific Laboratory during the period 1 July through 31 December 1976. The topics covered include optically pumped gas lasers, frequency calibration of the ¹⁴ CO ₂ laser, and microwave frequency shifting.		

DD FORM 1 JAN 73 1473 EDITION OF 1 NOV 65 IS OBSOLETE

UNCLASSIFIED

SECURITY CLASSIFICATION OF THIS PAGE (When Data Entered)

